

Nanocelluloses: Sources, Pretreatment, Isolations, Modification, and Its Application as the Drug Carriers by Sheilla Santoso

From Similarity check (check paper Jakad SPS)

Processed on 01-Mar-2022 11:34 WIB
ID: 1773576395

Word Count: 23883

Similarity Index	Similarity by Source	
8%	Internet Sources:	N/A
	Publications:	8%
	Student Papers:	N/A

sources:

- 1 1% match (publications)
[Jungang Jiang, Yeling Zhu, Feng Jiang, "Sustainable isolation of nanocellulose from cellulose and lignocellulosic feedstocks: Recent progress and perspectives", Carbohydrate Polymers, 2021](#)

- 2 1% match (publications)
[Ning Lin, Alain Dufresne, "Supramolecular Hydrogels from In Situ Host-Guest Inclusion between Chemically Modified Cellulose Nanocrystals and Cyclodextrin", Biomacromolecules, 2013](#)

- 3 1% match (publications)
[Yan Sun, Youlu Chu, Weibing Wu, Huining Xiao, "Nanocellulose-based lightweight porous materials: A review", Carbohydrate Polymers, 2021](#)

- 4 1% match (publications)
["Cellulose-Based Superabsorbent Hydrogels", Springer Science and Business Media LLC, 2019](#)

- 5 < 1% match (publications)
[Sujie Yu, Jianzhong Sun, Yifei Shi, Qiangqian Wang, Jian Wu, Jun Liu, "Nanocellulose from various biomass wastes: its preparation and potential usages towards the high value-added products", Environmental Science and Ecotechnology, 2020](#)

- 6 < 1% match (publications)
[Jian Li, Yujia Wang, Lei Zhang, Zhaoyang Xu, Hongqi Dai, Weibing Wu, "Nanocellulose/Gelatin Composite Cryogels for Controlled Drug Release", ACS Sustainable Chemistry & Engineering, 2019](#)

- 7 < 1% match (publications)
["Nanocellulose", Wiley, 2019](#)

- 8 < 1% match (publications)
[Emanuela Sgreccia, Riccardo Narducci, Philippe Knauth, Maria Luisa Di Vona, "Silica Containing Composite Anion Exchange Membranes by Sol-Gel Synthesis: A Short Review", Polymers, 2021](#)

- 9 < 1% match (publications)
[Korbinian Löbmann, Anna J. Svagan, "Cellulose nanofibers as excipient for the delivery of poorly soluble drugs", International Journal of Pharmaceutics, 2017](#)

- 10 < 1% match (publications)
[Sina Salimi, Rahmat Sotudeh-Gharebagh, Reza Zarghami, Siok Yee Chan, Kah Hay Yuen, "Production of Nanocellulose and Its Applications in Drug Delivery: A Critical Review", ACS Sustainable Chemistry & Engineering, 2019](#)

- 11 < 1% match (publications)
["Handbook of Nanocellulose and Cellulose Nanocomposites", Wiley, 2017](#)

- 12 < 1% match (publications)
[Jie Jiang, Wenbo Ye, Liang Liu, Zhiguo Wang, Yimin Fan, Tsuguyuki Saito, Akira Isogai, "Cellulose Nanofibers Prepared Using the TEMPO/Laccase/O System", Biomacromolecules, 2016](#)

- 13 < 1% match (publications)
[Jindrayani Nyoo Putro, Valentino Bervia Lunardi, Felycia Edi Soetaredjo, Maria Yuliana et al, "A Review of Gum Hydrocolloid Polyelectrolyte Complexes \(PEC\) for Biomedical Applications: Their Properties and Drug Delivery Studies", Processes, 2021](#)

- 14 < 1% match (publications)
[Habibi, Youssef, "Key advances in the chemical modification of nanocelluloses", Chemical Society Reviews, 2014.](#)

- 15 < 1% match (publications)
[Nurhasni Hasan, Latifah Rahman, So-Hyeon Kim, Jiafu Cao, Andi Arjuna, Subehan Lallo, Byung H. Jhun, Jin-Wook Yoo, "Recent advances of nanocellulose in drug delivery systems", Journal of Pharmaceutical Investigation, 2020](#)

-
- 16 < 1% match (publications)
[Wan Hazman Danial, Nur Fathanah Md Bahr, Zaiton Abdul Majid. "Preparation, Marriage Chemistry and Applications of Graphene Quantum Dots–Nanocellulose Composite: A Brief Review", *Molecules*, 2021](#)
-
- 17 < 1% match (publications)
[Lars H. Kruse, Austin T. Weigle, Mohammad Irfan, Jesús Martínez-Gómez et al. "Multiple routes of functional diversification of the plant BAHD acyltransferase family revealed by comparative biochemical and genomic analyses", *Cold Spring Harbor Laboratory*, 2021](#)
-
- 18 < 1% match (publications)
[Vimal Katiyar, Prodyut Dhar. "Cellulose Nanocrystals", *Walter de Gruyter GmbH*, 2020](#)
-
- 19 < 1% match (publications)
[Gorgieva, Trček. "Bacterial Cellulose: Production, Modification and Perspectives in Biomedical Applications", *Nanomaterials*, 2019](#)
-
- 20 < 1% match (publications)
[Alain Dufresne. "Nanocellulose", *Walter de Gruyter GmbH*, 2017](#)
-
- 21 < 1% match (publications)
[Estefanía Álvarez-Castillo, José Manuel Aguilar, Carlos Bengoechea, María Luisa López-Castejón, Antonio Guerrero. "Rheology and Water Absorption Properties of Alginate–Soy Protein Composites", *Polymers*, 2021](#)
-
- 22 < 1% match (publications)
[Polysaccharides, 2015.](#)
-
- 23 < 1% match (publications)
[Yee Yee Khine, Martina Heide Stenzel. "Surface modified Cellulose Nanomaterials: A Source of Non-Spherical Nanoparticles for Drug Delivery", *Materials Horizons*, 2020](#)
-
- 24 < 1% match (publications)
[Wei Liu, Haishun Du, Miaomiao Zhang, Kun Liu, Huayu Liu, Hongxiang Xie, Xinyu Zhang, Chuanling Si. "Bacterial Cellulose-Based Composite Scaffolds for Biomedical Applications: A Review", *ACS Sustainable Chemistry & Engineering*, 2020](#)
-
- 25 < 1% match (publications)
["Advanced Functional Materials from Nanopolysaccharides", *Springer Science and Business Media LLC*, 2019](#)
-
- 26 < 1% match (publications)
[Ansar Karimian, Hadi Parsian, Maryam Majdinia, Mahdi Rahimi et al. "Nanocrystalline cellulose: Preparation, physicochemical properties, and applications in drug delivery systems", *International Journal of Biological Macromolecules*, 2019](#)
-
- 27 < 1% match (publications)
[Kai Hua, Igor Rocha, Peng Zhang, Simon Gustafsson, Yi Ning, Maria Strømme, Albert Mühranyan, Natalia Ferraz. "Transition from Bioinert to Bioactive Material by Tailoring the Biological Cell Response to Carboxylated Nanocellulose", *Biomacromolecules*, 2016](#)
-
- 28 < 1% match (publications)
[Sven F. Plappert, Falk W. Liebner, Johannes Konnerth, Jean-Marie Nedelec. "Anisotropic nanocellulose gel-membranes for drug delivery: Tailoring structure and interface by sequential periodate–chlorite oxidation", *Carbohydrate Polymers*, 2019](#)
-
- 29 < 1% match (publications)
["Sustainable Polymer Composites and Nanocomposites", *Springer Nature*, 2019](#)
-
- 30 < 1% match (publications)
[Advanced Structured Materials, 2015.](#)
-
- 31 < 1% match (publications)
[Bejoy Thomas, Midhun C. Raj, Athira K. B., Rubiyah M. H., Jithin Joy, Audrey Moores, Glenna L. Drisko, Clément Sanchez. "Nanocellulose, a Versatile Green Platform: From Biosources to Materials and Their Applications", *Chemical Reviews*, 2018](#)
-
- 32 < 1% match (publications)
[Marta A. Teixeira, Maria C. Paiva, M. Teresa P. Amorim, Helena P. Felgueiras. "Electrospun Nanocomposites Containing Cellulose and Its Derivatives Modified with Specialized Biomolecules for an Enhanced Wound Healing", *Nanomaterials*, 2020](#)
-
- 33 < 1% match (publications)

34 < 1% match (publications)

[Kingshuk Dhali, Mehran Ghasemlou, Eugen Daver, Peter Cass, Benu Adhikari. "A review of nanocellulose as a new material towards environmental sustainability", Science of The Total Environment, 2021](#)

35 < 1% match (publications)

[Mehran Ghasemlou, Eugen Daver, Elena P. Ivanova, Youssef Habibi, Benu Adhikari. "Surface modifications of nanocellulose: From synthesis to high-performance nanocomposites". Progress in Polymer Science, 2021](#)

paper text:

polymers Review

2Nanocelluloses: Sources, Pretreatment, Isolations, Modification, and Its Application as the Drug Carriers

2Valentino Bervia Lunardi 1, Felycia Edi Soetaredjo 1,2, Jindrayani Nyoo Putro 1, Shella Permatasari Santoso 1,2, Maria Yuliana 1, Jaka Sunarso 3, Yi-Hsu Ju 4,5 and Suryadi Ismadji

1,* Citation:

16Lunardi, V.B.; Soetaredjo, F.E.; Putro, J.N.; Santoso, S.P.; Yuliana, M.; Sunarso, J.; Ju, Y.-H.; Ismadji, S. Nanocelluloses: Sources, Pretreatment, Isolations, Modification, and Its Application as

the Drug Carriers. Polymers 2021, 13, 2052. <https://doi.org/10.3390/polym13132052>

8Academic Editors: Denis M. Panaitescu **and** Adriana Nicoleta Frone **Received:** 26 May 2021 **Accepted:** 21 June 2021 **Published:** 23 June 2021 **Publisher's Note:** MDPI stays neutral with regard to jurisdictional claims in published maps and institutional affiliations. **Copyright:** © 2021 by the authors. Licensee MDPI, Basel, Switzerland. This article is an open access article distributed under the terms and conditions of the Creative Commons Attribution (CC BY) license (<https://creativecommons.org/licenses/by/4.0>)

1). 1 Department of Chemical Engineering, Widya Mandala Surabaya Catholic University, Kalijudan 37, Surabaya 60114, Indonesia; valentinolunardi70@gmail.com (V.B.L.); felyciae@yahoo.com (F.E.S.); jindrayoo@yahoo.com (J.N.P.); shella_p5@yahoo.com (S.P.S.); mariayuliana@ukwms.ac.id (M.Y.) 2 Department of Chemical Engineering, National Taiwan University of Science and Technology, No. 43, Section 4, Keelung Rd, Da'an District, Taipei City 10607, Taiwan 3 Research Centre for Sustainable Technologies, Faculty of Engineering, Computing and Science, Swinburne University of Technology, Kuching 93350, Sarawak, Malaysia; jsunarso@swinburne.edu.my 4 Graduate Institute of Applied Science, National Taiwan University of Science and Technology, No. 43, Section 4, Keelung Rd, Da'an District, Taipei City 10607, Taiwan; yhju@mail.ntust.edu.tw 5 Taiwan Building Technology Center, National Taiwan University of Science and Technology, No. 43, Section 4, Keelung Rd, Da'an District, Taipei City 10607, Taiwan * Correspondence: suryadiismadji@yahoo.com; Tel.: +62-31-389-1264 **Abstract:** The 'Back-to-nature' concept has currently been adopted intensively in various industries, especially the pharmaceutical industry. In the past few decades, the overuse of synthetic chemicals has caused severe damage to the environment and ecosystem. One class of natural materials developed to substitute artificial chemicals in the pharmaceutical industries is the natural polymers, including cellulose and its derivatives. The development of nanocelluloses as nanocarriers in drug delivery systems has reached an advanced stage. Cellulose nanofiber (CNF), nanocrystal cellulose (NCC), and bacterial nanocellulose (BC) are the most common nanocellulose used as nanocarriers in drug delivery systems. Modification and functionalization using various processes and chemicals have been carried out to increase the adsorption and drug delivery performance of nanocellulose. Nanocellulose may be attached to the drug by physical interaction or chemical functionalization for covalent drug binding. Current development of nanocarrier formulations such as surfactant nanocellulose, ultra-lightweight porous materials, hydrogel, polyelectrolytes, and inorganic hybridizations has advanced to enable the construction of stimuli-responsive and specific recognition characteristics. Thus, an opportunity has emerged to develop a new generation of nanocellulose-based carriers that can modulate the drug conveyance for diverse drug characteristics. This review provides insights into selecting appropriate nanocellulose-based hybrid materials and the available modification routes to achieve satisfactory carrier performance and briefly discusses the essential criteria to achieve high-quality nanocellulose. **Keywords:** drug delivery; drug release; functionalization; nanocellulose 1. Introduction Drug delivery technology (DDT) is a cutting-edge applied science for delivering drugs to specific targets. This technology regulates the absorption and release of therapeutic drugs via various drug carriers

to the desired organs, including subcellular organs, tissues, and cells, to improve human health [1]. DDT has advanced rapidly in the past few decades, enabled by various discoveries in various fields, including pharmaceutical, materials, and biomedical sciences. DDT development aims to improve therapeutic drugs' pharmacological activity and overcome various disadvantages of conventional therapeutic drugs such as drug agglomeration, biodistribution deficiency, low bioavailability, limited solubility, and insufficient selectivity to prevent the concurrent effects of therapeutic drugs. *Polymers* 2021, 13, 2052.

<https://doi.org/10.3390/polym13132052> <https://www.mdpi.com/journal/polymers> The majority of research studies on drug delivery technology revolve around developing materials suitable for drug delivery with desirable characteristics such as high drug adsorption capacity, targeted drug administration, controlled release, biocompatibility, and non-immunogenic and non-toxic effects that optimize therapeutic efficacy and eliminates side effects [2]. Many engineered nanomaterials have been studied for drug delivery applications [3]. Some nanomaterials have recently been undergoing development and clinical investigation; however, each nanomaterial has its various characteristics and limitations, challenging the researcher in creating a suitable drug delivery system. Natural-based polymers have drawn considerable attention as suitable biomaterials for numerous applications in drug delivery systems. Various nature-based

4 polymers such as polysaccharides (cellulose, chitosan, hyaluronic acid

, pectins, alginate, cellulose ethers), proteins (silk fibroin and collagen), and peptides have been identified as promising biomaterials for drug delivery systems given their biocompatibility, processability, and characteristics (e.g., nanoparticles, hydrogels, aerogels, tablets, and so on) that can be regulated by modifying various polymer functional groups such as amino groups, carboxyl groups, and hydroxyl groups [4]. The current development of these mentioned various polysaccharides, proteins, and peptides for

4 drug delivery systems have been well-reviewed

elsewhere [4–7]. Several natural polymers have been shown to have a higher affinity for cell receptors and modulate cellular processes such as adhesion, migration, and proliferation. These advantages make these natural polymers attractive for effective and high-efficiency drug delivery systems [8]. They can also be degraded in the presence of in vivo enzymes, which ensures their ability to create responsive local delivery systems. However, only polysaccharides and proteins have been extensively studied in drug delivery systems (DDS). These natural polymers have unique characteristics in each tissue and have identical characteristics in the extracellular skeleton. These characteristics support these natural polymers' utilization as drug carriers with insignificant invasive features [9–11]. Cellulose is the most abundant and commonly found natural polymer [12]. Its annual production is estimated at more than 7.5 · 10¹⁰ tons [13]. As a promising fuel and chemical precursor, cellulose has been widely utilized in various industries such as textile, pulp, paper, composite, and pharmaceutical excipients [2]. However, the development of cellulose-based materials as a direct molecule controller for drug adsorption and release had not been evaluated until the discovery of nanocellulose, which became a turning point for using carbohydrate-based nanomaterials in the field of drug delivery [14,15]. As illustrated in Figure 1, the publication on nanocellulose for biomedical engineering applications increases every year, especially for drug delivery applications. The increase in the number of publications on the utilization of nanocellulose for drug delivery systems is a strong indication of the potential application of this material in the future. The rapid development of nanotechnology and materials science has brought about nanocellulose as a potential drug carrier because of its extraordinary physicochemical and biological characteristics. Nanocellulose has a large surface-area-to-volume ratio, thus enabling more significant adsorption and therapeutic drug-binding capacity than other materials. With these properties, nanocellulose can facilitate drug release mechanisms and allocate drug delivery precisely to the target to drastically reduce drug consumption, leading to improved drug delivery system effectiveness [16,17]. Nanocellulose additionally exhibits other attractive characteristics

15 such as stiffness, high mechanical strength, biocompatibility, low

toxicity, lightweight, tunable surface chemistry, and renewability [11,18],

15 which are desirable for the design of advanced drug delivery

system. *Polymers* 2021, 13, x 3 of 49 (a) (b)

FFiiguurree11..TThheennuummbeerooffppuubblliccaattioonnssinnththeearreeaaoffnnaannooceelllululolosseeannddnnaannooceelllululolosseefc
bbyySSccooppuusffroomm22001100--uunnttiilrreeceenntt((1100JJuunnee22002211))

((aa));;ddaattaarreeppreesseenntaattioonnoffaannnuuaallppuubblliccaattioonnoffnnaannooceellllululoolosseeiinnvvaariioouuss
ccaatteeggooorriieess off bbiioommeeddiiccaall

eennggineeeri,ninggwwithhinthetheelaslstdedcaedcaedse(bs)

(bd)a;daaataanaalysailsypsiesfpoerrmfoerdmoendSoconpSucsoupsuinsgutshinegtetrmstneramos-

cellulose and nanocellulose for x (x refer to biomedical engineering, drug delivery, tissue engineering, wound healing,

niampolcaenlltus,loAsnetiabnactnerainalo/caenlliumloicsreofboiar",.xa"nd(xcarredfeiorvtaosbcuiolamr)e.dical

engineering, drug delivery, tissue engineering, wound healing, implants, Antibacterial/antimicrobial, and

cardiovascular). Nanocellulose can be utilized as either carrier or excipient for broad application in

drugNdaenliovceerlylusossteemcasubcehuatsilimzeicdroapsaeritichleers,ctaarbrietrs,ohyredxrcroigpeelsn,tafeorrogberlosa,dregapulpalticnagtinona
innodpraungticdlesli,vaenrdy msyesmtebmransseucdhruags

dmeilcivroepryarstycsitem,tsa[b19e]t.sN,hayndorcoeglleullo,saehroagseblese,nremgualnautifnagc-

nttuuarreeoddpaoonrttictthleesla,laabbnoodrramatotoermryabanmadndieninddruusgtrtdiraielsilvcsaeclaeyl,esi,.yeis,.e.te.r,marnasgn[1gn9ign].

inn thhreeee
ddiiffieerrenntffoformmssasannaoncorcyrstastlallinieceeclleullousloes(eN(CNCC),Cn)a,nnoafnboefirbceerllucelollsuelo(NseFC(N),FaCn)d,
abndactberaictatenriaanloncaenloulcleolsleu(oBsNeC(B)N[2C0]).
[S2e0v].eSraelvreecaelnrtreesnetarrecsheaamcdhraenvdierwevaiertwiclaersthcalevsehcaovme-
cpormehpernehsievnesiyevolvveorvveierwievedwethperpocroeces,sse,xetxrtarcactiotino,n, chchaaraccteterrizaatioonn,,aanndd
aappplliiccaattioonnss ooff
nnaannoocceellluulloosseeaannddthheeiirmmooddiiffieedssttrruuccttuurreessinindrruuggddeelliviveerrysystetemms[1[122,1,177,2,211—
2244].
TThheeddruggbbiinndiinngaannndthheerleeeaaasettiimeeooffnaannoocceellluulloossee--
bbaasseedddrruuggssvvaaryydeeppeennndiinng onn thhee nnaannoocceellluulloossee
ccoonnffigguurraattioonn,, thheeraappeeuutticcaall iinggrreeddiieentt'ss aacctiivviityy,, thhee
pprrroodduuccttiioonn method, and thhee
modification[2[255,2,266].ThTehreerfeofroer,en,annaoncoeclleullousloesies
aisparopmroimsinisingcarciaerrifeorr
fvoarvriausodursudgrudgeliveirvyesryssteymstsemuscschuacshoarsaolraadmadinmisitriastiroanti,oonp,hotphatlmhailcmdircudgrudgelidveelrivye
intratumoral administration, transdermalddruugg delivery, topical administration, and local drug delivery.
This review

7 provides a comprehensive overview ooff the preparation procedures ooff
nanocellulose and the

various effects on drug formulation and delivery. Three types ooff nanocelluloses and a brief description of
their synthesis processes are discussed aattthe beginning of this review.
Subsequently,t,hteheeffeefctetsctosf orafwramwamteraitaelrsiaalnsdatndhe syntshyensitshpesrios-
proceosns othnethe characteristicofcs tofhethreesureltsaunttant
nanocellulosareeadreisduisscsuedss.eTdh.isThisthisenthfionl- floolwoewdebytyhethethe applicatioonoff
nanocelluloseoto varioudsrdurgug delivery systems. 2. Conversion of Cellulose into Nanocellulose and Its
Characteristic Cellulose isisththe most abundant natural polymer glogblaollbyaallnyndsda
risenaerweanbelweasboulercseoaurncde
easnsdenetsiaslenratwialmraawtermiaalfteorriavlaforiorusarinioduussitridesu.sCtreiellsu.ICoseelluisloasceruiscialrcrucocnisatitucioennstictoumenptocu
fpoorupnladntos,rmlpaarintse,amnaimrinales,aanligmaea,lsfu,anlggia,eb,afcutnergia,,baancdtearmiao,aenbdaea[m12o]e.blnae[181328].,Flne1n8c3h8c
AchnesmelmistAPnayseelnmdeisPcaoyveenreddisacnodveisreodlataenddcieslolulaltoesde
fcreollmlopslaentfrofimbeprsaunstinfibenstruicsaingcjdnaintrdic
daectiedrmanindeddeittesrcmheinmedicaitstscrhuectmuircea.ITshreuprctiumrea.ryThsoeupcriemsoarfyceslolulucroeseeasorfe
cpelallnutofisbeerasrewpithanant hfibgehrscewllithlosaehciognhtecnellt,usluosche
caosnctoentot,nsu(ccohnatasincointtgonm(ocroenthaainn9g0%moerleluthloasne
9c0o%ntecnellt)u[2o7s]e
acnodntwenotd[2(7u)patnod5w0%oocdel(luuplostoe).50O%thceerlluculmospeo).uOndtheseruccohmapsohuenmdiscsluluchloasae,
hliegmninice,plueclotisne,,
alingdnwn,apxeacrteina,lsaondprwesaeaxnat;rethaelysocapnrebseenret;ctohveeyreccanduberimegcothveerseepadruartiionng
pthreocseespsa.ration pro- cess. Polymers 2021, 13, x 4 of 49 Polymers 2021, 13, 2052 4 of 47 Recently,
various agricultural wastes with high cellulose content were explored as a
sourcReeocfencettlyu,vloasrei,osuuscahgarsicouilltupraallmweamstpetsywfrutuhithbiguhnccheellsu(I0osPeEcFoBn)te[2n8t]w,pearelmexapnldorbeadnaasr
fsroounrdes,opfacsesllionofsreu,itsupchelaswoaisltpea[Im29]e,mbpagtyasfsreu,itwbnueacthestsr(aOWP,ErFicBe)
s[2tr8a]w,p,ablmamabnodobsatnaalknsa, hfreomndps,bpaarkss,iponoftrautoit
tpebeelrws,amsteu[2b9e]r,rbyabgaarsks,e,hwemhepatasvtricaewl,,
raincdessturagwar,bbaemetso[03s0t]a.ICkse,lhuelmospe dbaerrkiv,epdoftraotomtuthbeesres,nmonu-
lpleamrnytpbraercku,rhseomrspcaanvihcaevl,eaandmsoulegcaurlbaerestsru[3c0tu].reCseilmulluloasretodethriavteodf
pfroamntcheellsuelonsoen.-
Hploawntevperre,ctuhresomsaicnadhifhaevreenacemisoltehcautlmaruscthrulcetsusrheesmimicellallrutloostehaort
olifgnianlants pcerleluselonstei.nHtohweseevenro,nth-pelmanati-nbadsieffderpenreccueirsstohrast;
mhiugchherless hemicelclounlotesnetowrlitghnminuischprleowenetr iinntphuersietinesonca-pnlabneto-
bbatsaeindepdrfrcoumsrothsrse;sheipgrheecrucreslolurlo.se content with much lower impurities can
blenotbertaminseodfcrhoemmitchaelssetpurcetcuures,ocresl.ulose is composed of a linear
homopolysaccharide consilnt toefm β -sDo-gflcuhecompyicraalnsotsruecutunriets,
ceentliurleolsyeciosncdoempseodseadnodfbaolnindeeadr hthormooupgpholy β s-a1c,4c-hgalyricdoe-
scoidnesilnitokfa β ge-De-
(gFluigcuorpey2r)a.nTohseesutnruitcsteunrteirfeolunycdonatdioennsoefdtahnedceblolundloesdetnertowuogrkh β -
s1a,4r-rgalngceodsibey
alinchkaaginesgl(uFcigosueredi2m).eTthcoemstpruicstinugretwfoounandhaytdornouofstghluccoeselelusi(oAsGe)ndetewfionrekdiassacreralonbgiodseb
(cFhiagiunrgel2u)c.oTsheedriamwemrcatmerparliarilointngthetwporeatrhaytmdreouuts(cghluemcoisceaso(ArmG)ecdehaffiniecda)jasofcceeellolublooosse
a(Fffigecutreth2e).cTelhuelroaswecmhaitnerlianlgotrthaendprtehturesaltemadento(cmhoelmecicualalrorwmeiegchhtavnacraial)tioofnc.eTlthuelonsuen
oafffeAcGtthuenicelstliunloasechchchahianleinsgkthnoawndntahsutshieeapdolyommeorizecautiloanrwedegigrehetv(PaDria).tiTohne.TvhaeluneuomfbP
foofrAcGelluunloitsseinpoeawcdhechrvaianriesskfnroowmn1a0s0thtoe
3p0o0lyumneirtsizaantidonadroegunrede 2(P6D,5)0.0ThfoervcaellulueloofpePDpufolpr [c3e2ll]u.ITohsee
PpDowdaleurevfaorricsefflruolmos1e0f0rotmo3c0o0ttuonitiss
1a5n,d00a0r,oaunnddw26o,o5d00isfoarppcerlolulximosaelepluy1p0[,03020]. T[3h3e].PD value for cellulose
from cotton is 15,000, and wood is approximately 10,000 [33]. FFIgguurree 22.. SSchcheemmaatiticc ooff
cceeellluulloossee pprroodduuccttiioonn ffrroomm wwoooodd pplaanntt aanndd ssttrruuccttuurraall
cchheemmiisstryy ooff eexxhhiibbiittinngg aarrrraannggeemmenntt bbeetwwiixxtt iinnddiivviiduuuall
ffibberrrs.. Each cellulose monomer contains three reactive

26 hydroxyl groups in the repeating chemical structure of the β -D-
glucopyranose

unit. In the same chain, these

4hydroxyl groups can make hydrogen bonds with the

adjacent β -D-glucopyranose units. At different Each cellulose monomer contains three reactive

26hydroxyl groups in the repeating chemical structure of the β -D-glucopyranose

unit. In the same chain, these

4hydroxyl groups can make hydrogen bonds with the

adjacent β -D-glucopyranose units. At different chain locations, the bonds present are intramolecular and intermolecular hydrogen bonds responsible for the crystal arrangement, determining the cellulose's physical characteristics. Based on molecular orientation and hydrogen network between molecules and intramolecular, cellulose is classified into different types, i.e., I, II, III, IIII, IVI, and IVII. For details about the classification of cellulose, the reader can refer to the work of Moon et al. [34]. Some of the cellulose characteristics are mainly represented by hydrogen linkage coordination [35,36]. Structurally, the

4cellulose is a linear chain polymer with a rod-like

configuration, aided by the glucose residues' equatorial conformation that is intensely aggregated together with the lateral size 3–5 nm [36]. Primary chains of cellulose, especially polysaccharide chains, are found on the secondary walls of plants arranged in a parallel configuration. The cellulose's basic fibers have a cross-sectional diameter between 10–450 nm with a length of several micrometers that depend on the diversity of material sources [37]. Moreover, the elementary fibrils were arranged into large pack units called microfibrils, further foregathered into fibrils [13]. There are regions within the cellulose fibrils where the cellulose chains are organized into a highly crystalline structure with a length of 50–150 nm and disordered amorphous regions with 25–50 nm [34]. The cellulose chains construct the crystalline regions through Van der Waals forces, strong intra- and intermolecular hydrogen linkage, and

22 β -1,4-glycosidic bonds. In

contrast, amorphous regions are built up through the deficiency of hydrogen bonds in the crystalline region. The crystalline and amorphous regions in cellulose may vary depending on various sources. The crystalline constituent within cellulose fibers can be refined through various chemical treatments by destructing and removing the disordered amorphous or para-crystalline regions. The purified crystal fragments with particle sizes on the nanometer scale are called nanocrystalline cellulose (NCC) (Figure 3). Different shapes of NCC are present such as needle and elongated rod-like shape or spindle-like shape with high stiffness of crystalline fragments [38], which are reported as cellulose whisker [39], nanowhisker [40], nanorod [41], and spherical nanocrystal [42]. Polymers 2021, 13, x 6 of 49 Figure 3. Schematic representation nanocrystalline cellulose fabrication by chemical treatment (a) transmission electron

mFiigcursec3o.pSych(TeEmMat)icimreapgresseonfarotido-nlikneancoeclrluylsotsaellinnaenocelrluylsotasels[a3b8r]i.caretipornbtyedchweimthicpaelrtmreiaistsmioenn;t(r(aan)stmrainssmioinsseiloencterloenctrn

15microscopy (TEM) images of rod-like cellulose nanocrystals [38], reprinted with permission

; transmission electron micros- ccroopsco(pTyE(MTE)Mim)aimgeasgoefs

coefficientlousleosneannaonwohishkisekrerreprepiritnedtedwwiththepremrmisissioinonfrromm[2[255]].CCoopyyirrigghtt

@22001199EEllsseevieerr BB..VV.; ((bb)) transmission electron microscopy (TEM) images ooff spherical

cellulose nanocrystal reprinted with permission from [43]. Copyright © 2018 Elsevier B.V.). Attoopp-

ddoowwnpprroocceessshaassbbeeeennaapppllieeddfloorNNCCCCpprroodduucttiioonninnwwhhiicchhallaarrggeeunniittooff

cceellluulloseeffibberss((ccmm))iissddiissinntteeggraatteeddtthhrroouughhchcheemmiccaalloormmeecchhaanniccaalltreeaattmmeennttiinttoof unniittsooffnaannoocceellluullosee((nnmm))

[4444]..NNCCCC"sscchheemmiccaallssttrruuccttuurreeiissccoonssttrruucctteeddbbyiinnttraa--aanndd

iinntteerrmmoolleccuullaarrhyddrooggeennliinnkaaggeeooffce.eillluulloseenmaacccroommooleeccuuleesswiitthahhiighghccrrysstaallliinnit vvaallueevvaaryyininggfrromm5454toto888%8%

[4[54]5.]N.NCCCCs.psapratirtlieclseizeizeeddeepenpdensdosnothnetohreigoirngoifnthoetcheellucelollsue-

sloosuercseosu,wrcietch,tweithdiathmeedteiramanedtelrenagndthlhteyngictahllyypvaicrayliinygvaerthywnegeen5etawnede3n0nmandan3d0bnemtwear

1b0e0twaneedn510000namnd.r5e0s0pencmti,vreelsyp[e4c6t]v.eTiyhu[4s,6]N.TChCush,NavCeCbsehcoavmebaencoamterraactvaetrcaactndiviedaca

drug carriers, given their outstanding physical and chemical properties [21,47,48]. date as drug carriers,

given their outstanding physical and chemical properties [21,47,48].

11Cellulose nanofiber (CNF), also known as cellulose

nanofibril, micro-fibrillated cellu-

11 Cellulose nanofiber (CNF), also known as cellulose

nanofibril, micro-fibrillated cellulose,

4 nano-fibrillar cellulose, nano-fibrillated cellulose

, or cellulose microfibril, has a similar structure,

4 nano-fibrillar cellulose, nano-fibrillated cellulose

, or cellulose microfibril, has a molecule structure to NCCs with nano-size particles. Similar to NCC, CNF can also be pro- similar molecule structure to NCCs with nano-size particles. Similar to NCC, CNF can Polymers 2021, 13, x 7 of 49 also be produced from various cellulose sources. However, the morphology and crystallinity of NCC and CNF are the unique features that differentiate these two cellulose-based

... strongly influenced by mechanical treatment and defibrillation [49].

Scanning electron microscopy (SEM) images of nano-fibrillar cellulose (NFC) and nano-fibrillated cellulose (NFC) ...

Figure 4 presents an illustration of CNF extracted from cellulose fragments via mechanical defibrillation. The exerted force fractures the cellulose fibrils along

... along the microfibrils. The exerted force fractures the cellulose fibrils along

Microbial cellulose (MC), bacterial nanocellulose (BC), and bio-cellulose (BC) have been used as the other terms

... bacterial nanocellulose (BC), and bio-cellulose (BC) have been used as the other terms

... bacterial nanocellulose (BC), and bio-cellulose (BC) have been used as the other terms

... bacterial nanocellulose (BC), and bio-cellulose (BC) have been used as the other terms

... bacterial nanocellulose (BC), and bio-cellulose (BC) have been used as the other terms

... bacterial nanocellulose (BC), and bio-cellulose (BC) have been used as the other terms

... bacterial nanocellulose (BC), and bio-cellulose (BC) have been used as the other terms

... bacterial nanocellulose (BC), and bio-cellulose (BC) have been used as the other terms

... bacterial nanocellulose (BC), and bio-cellulose (BC) have been used as the other terms

... bacterial nanocellulose (BC), and bio-cellulose (BC) have been used as the other terms

In terms of chemical composition, BC is indistinguishable from plant-based nanocellulose (e.g., NCC and CNF). However, BC has higher crystallinity (up to 84–89%) with fewer amorphous regions than NCC and CNF. Moreover, BC contains fewer

impurities and contaminants such as hemicellulose, lignin, and pectin, mainly found in plant-based nanocellulose. BC is a biocompatible material with non-cytotoxicity and non-genotoxicity for biomedical applications, especially drug delivery [60]. BC synthesis does not involve a complicated process such as mechanical and chemical treatment to cleave the hemicellulose or lignin within the lignocellulosic biomass, thereby allowing high cellulose purity. BC's properties can be modulated by various techniques such as substrate manipulation, culture condition and operation parameter, and proper bacterial strain selection [17,54]. In contrast to NCC and CNF, BC provides unique characteristics such as high crystallinity of nanocellulose (84–88%) and polymerization grade, high water uptake capacity (exceeding

19100 times of its weight), large surface area (**high**)

aspect proportion of fiber), outstanding

19tensile strength (Young modulus of 15–18 GPa

), flexibility, foldability, moldability, mechanical stability, and high porosity [60]. A summary of the characteristics of various types of nanocellulose is listed in Table 1. Table 1. Summary of the characteristics of various types of nanocelluloses. Types Parameter Nanocrystalline Cellulose (NCC) Cellulose Nanofibers (CNF) Bacterial Cellulose Cellulose whisker, cellulose Common names nanowhisker, cellulose nanowire, and cellulose nanorod or spherical cellulose nanocrystals Cellulose nanofibril, microfibrillated cellulose, Nanofibrillar cellulose, Nanofibrillated cellulose, and cellulose microfibril Microbial cellulose (MC), bacterial nanocellulose (BC), and bio-cellulose (BC) Morphological structure Needles like shape, elongated rod-like shape, and spindle shape Smooth, extended, and flexible chain Twisted ribbons like shape Structure of Nanocellulose Crystalline domains amorphous and crystalline domains Crystalline domains Chain Length ≥ 500 500–15,000 4000–10,000 Crystallinity (%) 54–88 - 84–88 Other Impurities and contaminant Possible to contain hemicellulose, lignin, and pectin Possible to contain hemicellulose, lignin, and pectin Contain no hemicellulose, lignin, and pectin Size (Length and Diameter) Diameter:

315–30 nm and Length: 100–500 nm Diameter

: 1–100 nm and Length: 500–2000 nm Diameter 20–100 nm and several micrometric lengths Process System Top-down system Top-down system Bottom-up system Tensile strength (Gpa) 7.5–7.7 [34] 13 0.2–0.3 Modulus Young (Gpa) 110–220 [45] Approximately 15 18–20 [60] Density (gr/cm³) 1.6 [61] 1.42 1.1 Characteristics Homogenous nanorod form, exceptional aspect ratio (length to diameter), appreciable specific surface area (SSA), biocompatibility, liquid crystalline attribute, inferior breaking expansion, high young's modulus, hydrophilicity, outstanding mechanical stiffness, tunable surface characteristic due to the reactive hydroxyl group and low density Extended length with excellent aspect proportion (length to diameter), superlative surface area, hydrophilicity, biocompatibility and adjustable characteristic through surface modification afforded by high extensive of hydroxyl groups in CNF. High crystallinity of nanocellulose (84–88%) and polymerization grade,

19high water uptake capacity (exceeding **100 times of its weight**), remarkable surface area (**high**)

aspect proportion of fiber), outstanding tensile strength (young modulus 15–18 Gpa), and flexibility, foldability, moldability, mechanical stability, highly biocompatible material, non-cytotoxic, un-genotoxic and high porosity Based on the previous discussion, cellulose can be subjected to a mechanical, biological, and chemical treatment to produce three different NCs, i.e., nanocrystalline cellulose, cellulose nanofibrils, and biological cellulose. They are classified based on various aspects such as morphology, particle size, crystallinity, nanocellulose structure, extraction techniques, and cellulose sources [56]. Moreover, other important factors such as interfibrillar arrangement, microfibril inclination, chemical constituent, cell dimension, and defects can also vary depending on the cellulose sources [62]. Among all the mentioned characteristics, mechanical strength is essential in the drug delivery field [63]. As summarized in Table 1, NCC possesses a high modulus young, up to 220 GPa, which is higher than glass (86 GPa) [61] and kevlar KM2 fiber (88 GPa) [45]. Furthermore, the mechanical stiffness of NCC can reach up to 7.7 GPa, which is higher than 302 stainless steel (3.88 GPa) [45] and kevlar KM2 fiber (1.28 Gpa) [45]. 3. Sources and Pretreatment of Raw Materials for Nanocellulose Productions In general, the production of nanocellulose (NC) consists of three steps: (1) Finding the suitable sources, (2) raw material pretreatment, and (3) NC extraction. The raw material's source and type influence the physical and chemical properties and the NC product's yield. Currently, most nanocellulose sources utilize high-quality biomass such as cotton, wood pulp, and dissolving pulp, which comprises the high cellulose content. However, in response to recent essential issues, such as the

5depletion of non-renewable energy and increasing global temperature, **the** researchers realized **the**

development of waste-based biomass as a feedstock for the production of nanocellulose. Various types of biomass waste, including forest residues, algae, agricultural, and industrial by-products, appear as potential

18raw materials for nanocellulose production. In terms of

chemical composition, each category of biomass waste

22 is primarily composed of cellulose, lignin, hemicellulose, pectin, and

other minor substances with different physical and chemical characteristics [64]. Agricultural and forest residues have similarities in their chemical composition, but lignin composition in agricultural waste is significantly high, while the cellulose content in forest residues is higher than in agricultural waste [64,65]. Among all of the waste-based cellulose sources, the nanocellulose extraction from industrial waste seems more complex since the chemical and structural composition of feedstock is variable and crucially depends on the residue types. The various impurities (e.g., hemicellulose, lignin, wax, and pectin) act as a structural barrier that hinders the accessibility to the cellulose material for the extraction process [22]. Therefore, pretreatment is necessary to remove the cellulose framework's impurities, permitting the aperture of the material framework to expedite cellulose microstructure access. Moreover, removing impurities is also beneficial to reduce the consumption energy of mechanical treatment for cellulose disintegration [66]. Another objective of raw material pretreatment is to regulate the biomass structure and size and overcome the plant cell wall recalcitrance. The pretreatment is generally divided into four categories such as physical (milling, grinding, microwave, ultrasound, etc.), chemical (dilute acid, mild alkali, TEMPO mediated oxidation, organosolv, and ionic liquid), biological (fungi, bacterial, and archaeal), and physicochemical (steam explosion, liquid hot water, wet oxidation, etc.) [67]. The effectiveness of the biomass pretreatment process depends on pH, temperature, type of catalyst, and pretreatment time. Selecting the appropriate pretreatment would allow avoiding the structure disintegration or loss of cellulose, ensuring low cost, and minimizing energy use to reduce toxic and hazardous waste [68]. The chemical pretreatment process is considered the most efficient and economically feasible for the disintegration of biomass with low pretreatment severity. However, chemical pretreatment is non-environmentally friendly and requires a wastewater treatment process [69]. Physical pretreatment is environmentally friendly and scarcely generates hazardous or toxic substances, but the major disadvantage lies in its high energy consumption, which is generally higher than chemical treatment [70]. Biological treatment is widely known as an eco-friendly process, operates under mild conditions, and consumes a lower energy amount. However, long pretreatment duration, low conversion, and carbohydrate loss tendency throughout pretreatment remain the main challenges of biological pretreatment by the microorganism [71]. Physicochemical pretreatment using a combination of chemicals and high temperature or pressure in extreme conditions can effectively escalate biomass degradation. Nevertheless, high energy input is required, which translates to high operation costs for this method. Proper pretreatment of cellulosic fibers can improve the hydroxyl group's accessibility, inner surface enhancement, crystallinity alteration, and fracture of the

4 intra and inter hydrogen bonds of cellulose, leading to the increased

fibers reactivity [72]. Detailed pretreatment of cellulose-based raw materials has been thoroughly discussed elsewhere [73]. The integrated pretreatment strategy of lignocellulosic waste biomass comprising two or more pretreatment stages increases the pretreatment process's effectiveness, product characteristics, and versatility of composition in extracted cellulose. An additional process that adds more steps to cellulose purification is highly undesirable [74]. For instance, de Carvalho Benini [75] performed alkaline treatment coupled with multiple stages of bleaching pretreatment followed by sequential dilute acid hydrolysis to increase the efficiency of impurities removal (e.g.,

10 starch, hemicellulose, and lignin/pectins) from the cellulose framework.
Similarly, Wijaya et al. [29] combined alkaline and bleaching

treatment to obtain higher purified cellulose from passion fruit peel. In a different study, Maciel et al. [76] obtained the

10 soluble and insoluble lignin after alkaline

treatment reached 60 and 75%, respectively. The summary of the pre-treatment strategy of waste-based nanocellulose sources is presented in Table 2. Table 2. Summary of waste-based sources for nanocellulose production and its characteristic. Waste Residue Nanocellulose Isolation Technique Sources Pretreatment Treatment Nanocellulose Characteristics References WASTE BASED FOREST RESIDUE Birch and Spruce sawdust Hot water treatment and subsequent delignification; Mechanical defibrillation TEMPO oxidation $\sigma = 171.6$ MPa; E = 6.4 GPa; CNF [77] Medium-density fiberboard Soxhlet extraction (Ethanol NCC and toluene), NaOH, and L:164.7 nm; W: 6.7 nm; CrI (%): [78] recurrent bleaching Acid hydrolysis (H₂SO₄) 71 Eucalyptus sawdust Hot water treatment, alkaline delignification, O₂ residual delignification, High pressure TEMPO-mediated homogenization Oxidation Davg: 41.0 nm; SSA: 60 m²/g; Y CNF (%) = 60 [79] Pinecone biomass Alkali treatment followed with acidification (NaClO₂:CH₃COOH) Mechanical grinding. σ : 273 MPa; E: 17 GPa; CNF CrI (%): 70%; D: 5–20 nm. [80] Logging residues Alkaline and bleaching pretreatment Acid hydrolysis (H₂SO₄) NCC L/D > 10; CrI (%): 86–93; TS (°C): 208.4–211 [81] Bamboo log chips Pretreatment with glycerol; and screw extrusion Mechanical refining/Milling treatment assisted by H₂SO₄ (0.15%) as a catalyst CNF D: 20–80 nm; CrI (%): 52.7%; Y [82] (%): 77.2 WASTE BASED ALGAE RESIDUE Cladophorales - TEMPO Oxidation; CNF W: 80 nm; SSA: 77 m²/g CrI (%): 93%; D: 80 nm; Excellent mechanical and rheological characteristics [83] NCC Red algae - Acid hydrolysis (H₂SO₄) L: 432 nm; W = 28.6 nm; L/D: 15.1; CrI (%) : 69.5; Yield: 20.5%; [84] TS (°C): 220 °C Green Seaweed Ulva lactuca Methanol pretreatment (Soxhlet extraction) followed by bleaching, alkaline pretreatment, and neutralization Acid

hydrolysis (H₂SO₄) CrI (%): 83; TS (°C): 225 °C NCC [85] Industrial kelp (*Laminaria japonica*) waste Two stages of bleaching NCC pretreatment (Chlorine L: 100–500 nm; D = 20–50 nm; dioxide followed with Acid hydrolysis (H₂SO₄) L/W: 5–20; Yield: 52.3%; TS [86] hydrogen peroxide) (°C): 240 °C Table 2. Cont. Waste Residue Nanocellulose Isolation Technique Sources Pretreatment Treatment Nanocellulose Characteristics References Dealginatate kelp residue From Giant Kelp (*Calrose* variety) Na₂CO₃ (2% wt) treatment, residual sodium alginate extraction by NaOH (2% wt); Ultrasonic irradiation; NaClO₂ (

50.7% wt) buffer solution bleaching treatment and delignification NCC Acid hydrolysis

(H₂SO₄) L: 100–500 nm; D = 20–50 nm; (°C): 120–180 °C; l = 120–480 nm L/W: 30–70; CrI (%): 74.5; TS [87] Chaetomorpha Acid hydrolysis (HCl) antennina Bleaching method followed with Ultrasonic irradiation CNF E = 0.9 Gpa; CrI (%): 85.02; Y = 34.09%; TS (°C) = 200–370 °C [88] Soxhlet Extraction (Ethanol: *Gelidium sesquipedale* Toluene) Bleaching treatment, delignification (5% KOH solution) Acid hydrolysis (H₂SO₄) followed with neutralization (NaOH) NCC L: 467–1650 nm; D = 18–29 nm; [89] L/W: ~40; CrI (%): ~70%; *Gelidium elegans* Alkali and bleaching pretreatment Acid hydrolysis (H₂SO₄) NCC L: 547.3 nm; D = 21.8 nm; L/W: [90] 25; CrI (%): 73%; TS (°C): 334 °C WASTE BASED AGRICULTURAL RESIDUE Waste sugarcane bagasse NCC Acidification and alkaline Acid hydrolysis (H₂SO₄) L: 170 nm; D = 35 nm; h = 70–90 pretreatment nm; CrI (%): 93%; TS (°C): [91] 249–345 °C

5Jute dried stalks Alkali treatment followed by steam explosion; sodium chlorite bleaching Acid hydrolysis (oxalic acid) followed by steam explosion

. CNF L: few micrometers D = 50 nm; CrI (%): 82.2%; E: 138 Gpa; TS (°C): 250–400 °C [92] Coconut husk Ultrasonic-aided solvent submersion. Delignification and Bleaching Pretreatment, followed by TEMPO-mediated Oxidation (TEMPO/NaClO/NaClO₂; pH = 4.8) Ultrasonication CNF (%) : 56.3%; TS (°C): 190–380 °C L: 150–350; D = 2–10 nm; CrI [93] Citrus waste Alkaline and Bleaching Enzymatic hydrolysis and Pretreatment ultrasonication CNF L: 458 nm; W: 10.3 nm; Davg = 10 nm; L/W: 47; CrI (%): 55%; [94] TS (°C): 190–380 °C Raw rice husk Size Reduction, Soxhlet extraction (toluene and ethanol); Acidification (NaClO₂ and CH₃COOH); and delignification (5% KOH) High pressure

5homogenization and high-intensity ultrasonication processes (500 W

,40 min). CNF 77.5%; L/D > 180; TS (°C): 323 L: 1800 nm; W: 10 nm; CrI (%): [95] °C One pot synthesis via Corn cobs - mechanochemical esterification $\sigma = 110\text{--}125$ MPa; E = 5.5 Gpa; CNF [96] D: 1.5–2.8 nm Delignification and three Kenaf bast fiber stage of bleaching Mechanical grinder CNF D: 1.2–34 nm; CrI (%): 82.52%; Y [97] pre-treatments (%) 60.25; TS (°C): 200–400 Passion Fruit Peels Alkaline and bleaching Acid hydrolysis (H₂SO₄) pretreatment followed with ultrasonication NCC L: 103–173.5 nm; CrI (%): 77.96%; TS (°C): 303.4; Y (%) : [29] 58.1 WASTE BASED INDUSTRIAL BY PRODUCT

5Olive industry solid waste Pretreatment including pulping and bleaching Acid hydrolysis

(H₂SO₄) NCC [98]

5Lime residues Autoclaving pretreatment High shear and high-pressure CNF D: 5–28 nm; CrI (%): 44–46

homogenization [99] Table 2. Cont. Waste Residue Nanocellulose Isolation Technique Sources Pretreatment Treatment Nanocellulose Characteristics References

5Recycled Tetra Pak Food Packaging Wastes Delignification and

Acid hydrolysis (H₂SO₄) bleaching pretreatment followed with ultrasonication NCC L/D: 10; CrI (%): 94.8%; TS (°C): L: 127–258 nm; D: 11.4–14 nm; [100] 204 Waste paper Deinking method and Acid hydrolysis (H₂SO₄) alkaline pretreatment followed with NCC [101] ultrasonication L: 271 nm Discarded cigarette Ethanol extraction, alkaline Acid hydrolysis (H₂SO₄) filters pretreatment, and bleaching pretreatment, followed with ultrasonication NCC L: 143 nm; W: 8 nm; CrI (%): [102] 96.77%; Y (%): 29.4 Recycled Paper Mill Sludge Ozonation pretreatment Acid hydrolysis (Maleic acid) NCC L: 2431 nm; W: 165 nm; L/D: 16.7 CrI (%): 77%; Y (%) : 0.8 [103] Citrus Pulp of Floater (CPF) Alkaline and bleaching pretreatment with autoclave Enzymatic hydrolysis n.d CrI (%):60 [104] Sweet lime pulp waste Blending and acid hydrolysis (H₂SO₄)

5Komagataeibacter europaeus SGP37 incubated in static intermittent fed-batch cultivation

BNC Y(g/L): CrI (%):89.6; TS (°C): [105] 348 Abbreviation: D: Diameter; L: Length; W: Width; TS: Thermal Stability; Y: Yield; L/D: Aspect Ratio; CrI: Crystallinity Index; l: Lateral size; σ : Tensile strength; E: Young Modulus. 4. Isolation of Nanocellulose 4.1. Isolation of Nano-Fibrillated Cellulose (NFC) Regardless of its

cellulose sources, NFC is mainly fabricated from cellulose pulp through mechanical treatment by breaking down the linkage of interfibrillar hydrogen [106]. The exerted mechanical force triggers the cracking phenomenon to

10 form a critical tension center in fibrous substances. The

development of NFC from fibrous material requires intense mechanical treatment with or without pretreatment. However, fibrous material's mechanical disintegration may cause pulp clogging, causing the fiber to agglomerate and require high energy to break it down. Thus, another pretreatment is required to overcome this problem. Several pretreatments have been introduced before the primary mechanical treatment to diminish the polymerization degree and debilitate the hydrogen linkage. These pre-treatments include mechanical refining, alkaline hydrolysis, solvent-assisted pretreatment, organic acid hydrolysis, 2,2,6,6-tetramethylpiperidine-1-oxyl (TEMPO)-mediated oxidation, enzymatic disintegration, periodate-chlorite oxidation, oxidative sulfonation, cationization, ionic liquid, carboxymethylation, deep eutectic solvents, and acetylation [17]. The earliest production of NFC was reported by Turbak et al. [107] and Herrick et al. [108]. They isolated NFC from wood via high-pressure homogenization (HPH). HPH exerted a mechanical force on cellulose fibrils driven by crushing, shear, and cavitation forces

10 in which cellulose pulp is transferred into the chamber through a small nozzle

to enable particle size reduction to the nanoscale of the cellulose fibrils [72]. Currently, the HPH is the most commonly utilized method for NFC production on an industrial and laboratory scale, given its simplicity, high efficiency, and lack of organic solvent requirements [109]. Furthermore, HPH enables high conversion of cellulose material toward CNF. High energy, high pressure, and long duration of the HPH process may also escalate the fibrillation degree. However, the difficulty of cleaning the equipment due to the blockage in the homogenizer valve is the major drawback of the HPH method [110]. Different processes have also been developed to produce CNF, such as micro-fluidization, micro-grinding, cryo-crushing, ultrasonication, mechanical refining, radiation, ball milling, blending, extrusion, steam explosion, and aqueous counter collision [111]. 4.2. Isolation of Cellulose Nanocrystal (NCC) According to the previous discussion, the main

15 difference between NCC and CNF lies in their structure, in which CNF comprises amorphous and

crystalline regions while NCC has high crystalline purity in cellulose regions. Therefore, the primary step in isolating NCC is to break down the disordered amorphous or paracrystalline regions that integrate the crystalline regions within cellulose fibrils. Initially, an NCC suspension was produced in 1949 from lignocellulosic biomass through an integrated alkaline and bleaching pretreatment and acid hydrolysis [13]. Acid hydrolysis remains the paramount process for NCC extraction. The crystalline part in cellulose fibers is not hydrolyzed because it has a high resistance to acids, although acids can easily hydrolyze the amorphous regions [112]. In this method,

34 sulfuric acid (H₂SO₄), hydrochloric acid (HCl), hydrobromic acid (HBr), and phosphoric acid (H₃PO₄) have been

extensively employed as the acid component to breakdown the amorphous region of cellulose. Following acid hydrolysis, the remaining free acid molecules and other impurities should be removed by diluting and washing with water using centrifugation and dialysis processes. Moreover, specific mechanical treatment like sonication may be needed to stabilize the NCC particles in uniform suspensions. However, the high tendency of corrosion, low recuperation rate, and high acid wastewater produced due to the high amount of water for the washing process for nanocellulose suspension neutralization become the significant drawbacks of the acid hydrolysis process [46]. To avoid excessive equipment corrosion and environmental issue, various nanocellulose isolation processes have been developed, such as extraction using ionic liquids, TEMPO oxidation, enzymatic, and others. Various researchers have carried out the combination and integration of various isolation processes to increase the isolation process's efficiency, such as enzymatic hydrolysis with TEMPO oxidation and enzymatic hydrolysis with ultrasonication [113]. Chemical treatment is crucial for NCC isolation, while mechanical treatment is the vital stage for CNF production. 4.3. Isolation of Bacteria Cellulose (BC) The selection of strains of microorganisms is a very crucial factor in the synthesis of BC. There are currently two main methods that have been used for BC production, i.e., static fermentation and submerged fermentation [54]. Static fermentation has been widely employed as an extracellular-based production route. In the static fermentation, a 3D network of gelatinous pellicles with high water content formed during the interspersing and intertwining of the ribbons structure form of BC, reaching a particular thickness corresponding to longer incubation time and causing the entrapment of bacteria cells and its further inactivity. The static fermentation produces BC with excellent crystallinity and mechanical strength, although prolonged cultivation and low productivity limit their industrial utilization. Furthermore, the BC layer's uneven thickness is produced due to the exposure of bacteria to uncertain conditions (nutrient, oxygen level, and cell distribution) throughout the growth cycle. Fed-batch strategies and submerged fermentation involving aeration and agitation fermentation have been introduced to overcome static fermentation's significant drawbacks. Submerged fermentation leads to higher BC productivity than static fermentation, which has been extensively utilized commercially. The cultivated bacteria are adequately exposed to oxygen, thereby generating a high yield of BC in the shape of small granules or pellets during aerated fermentation [114]. Moreover, agitation in the fermentation would result in a more homogeneous BC and oxygen evenly distributed to bacterial cells. However, the produced BC has lower crystallinity and mechanical strength than

static fermentation [115]. Several submerged fermentation issues such as the advancement of cellulose non- production strains [116], irregular shapes of BC granules or pellets, and physical character- istic modification of BC remain challenging for the researcher to overcome. In addition, excessive-high rotation speed and hydrostatic stresses may promote gluconic acid pro- duction by bacteria due to the accumulation of self-protection metabolism [117]. Several factors such as bacterial strains, fermentation medium carbon sources, growth condition, and its characteristic and yield should be evaluated carefully to choose the most suitable BC synthesis process selection approach. The summary of the recent studies of BC production is given in Table 3. Table 3. Recent study of bacteria cellulose production. Bacteria Cultivation Source of Carbon and Its Concentration Culture Medium Fermentation Conditions Yield (g/L) References Komagataeibacter xylinus K2G30 (UMCC 2756) Glucose 6.17 ± 0.02 Mannitol GY Broth Static; 28 °C; 9 days 8.77 ± 0.04 [118] Xylitol 1.36 ± 0.05 Komagataeibacter rhaeticus PG 2 Glycerol Glucose Sorbitol and Mannitol Hestrin–Schramm (HS) liquid media Static; 28 °C; 15 days ~6.9 ~4.05 ~1.65–3.41 [119] Komagataeibacter xylinus B12068 Glucose Sucrose Galactose Maltose and Mannitol Hestrin–Schramm (HS) liquid media Static; 30 °C; 7 days ~2.2 ~1.6 ~1.4 ~0.1–0.2 [120] Komagataeibacter Glucose medellinensis Sucrose Fructose Standard 2.80 Hestrin–Schramm (HS) Medium Static; 28 °C; 8 days 1.68 [121] 0.38 Date syrup ~1.15 glucose ~0.85 mannitol, Yamanaka ~1.4 sucrose ~1.45 food-grade

23sucrose ~0.7 Date syrup ~0.65 glucose

~0.7 Gluconacetobacter xylinus (PTCC 1734) mannitol, Hestrin–Schramm 150 rpm; 28 °C; 7 days, ~1.05 [122] sucrose ~1.5

23food-grade sucrose ~1.1 Date syrup ~0.9 glucose ~1

mannitol, Zhou ~

231.85 sucrose ~1.65 food-grade sucrose ~1

.15 5. Surface Chemistry of Nanocellulose for Drug Delivery Biocompatibility, biodegradability, and drug carrier capability to confine, control, and localize the drug release towards the target sites are desirable for nano-drug carrier formulation. The ability of nano-drug carriers to transport the drug and specify the sites for targeted drug release is influenced by the particle size, the surface charge, modification, and hydrophobicity. These aspects govern the nano-drug carrier interface with the plasma membrane and its diffusion across the physiological drug barrier [123]. Most NCs exhibit high specific surface area and negative interface charges as potential drug carriers, making them suitable as hydrophilic drug carriers. Therefore, the NCs' surface can be attached to the desired drug [124]. However, pristine NC cannot be used effectively as a drug carrier given its limited water solubility, moisture sensitivity, thermal instability, and lack of stability in various buffer solutions. Even though the pH adjustment of the environment can enhance the dispersibility of NCs, the scattering examination divulged the aggregation tendency of NCs, which translates to the colloidal instability of NCs. The size reduction obtained by converting cellulose into NC provides an exponential improvement of hydro- gen bonding that triggers the NC aggregation. This limitation can be made worse by the drug coordination, which is exposed on the NC exterior, consequently altering the dis- persibility and solubility [125]. Therefore, various surface modification and pretreatment fiber methodologies have been developed to overcome limitations and advance specific characteristics [126]. From a structural perspective, the three hydroxyl groups in each cellulose monomer are the most prominent characteristic that makes the NC surface reactive. The reactivity

20of hydroxyl groups influences the surface modification of

anhydroglucose units. It was reported that in the molecular framework of

20cellulose, the hydroxyl group at the sixth position behaves as primary alcohol

with a

29reactivity ten times larger than the other hydroxyl groups, while the hydroxyl group at the

second position has two-fold higher reactivity than that in the third position, both of which serve as secondary alcohols. This phenomenon manifests from the steric hindrance of each hydroxyl group, in which the hydroxyl group at the sixth position attached to the carbon atom that is connected to only one alkyl groups while the carbon atom that carries the hydroxyl groups in the second and third positions bonded to two alkyl groups [127]. Regarding the surface receptiveness of NC's hydroxyl groups, the addition of solvent and reactant may alter the group's receptiveness in diverse positions. De la Motte et al. [128] modified NCC through cationic epoxide 2,3-epoxypropyltrimethyl ammonium chloride (EPTMAC) by spray technique. It was revealed that the hydroxyl bunch receptiveness of cationic modified NC follows the order of OH-C6 = OH-C2 > OH-C3, which was validated through nuclear magnetic resonance (NMR). Nanocellulose surface modification for drug delivery was developed by modulating the NC hydroxyl groups. In general, the main

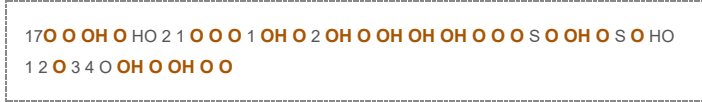
of cmhoemdiifccaaltmioondoiffncaatnionceollfunloanseociseltaubluoslaetisdainbuTlaabtleed4i.n Table 4.
 (a) Figure 6. Cont. Polymers 2021, 13, x Monocarboxylic Acid H3PO4 Hydrolysis Hydrolysis O



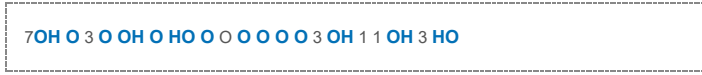
2 3 Dicarboxylic Acid OH OH of Phospated Nanocellulose of Phospated Nanocellulose Dibasic Form 1



(H3PO4/water); (H3PO4/Urea)



4 3 2 1 OH OH O H2SO4 Hydrolysis (H2SO4; ClSO3H; H2SO4/HCl) HO 1 O O 2 4 O O 4 O 1 2 OH 3 O 1 O 1



4 2 2



3 1 OH 2 2 Tricarboxylic Acid Hydrolysis (Citric acid) (b) FFiiguurree

66. SiSmimplpifliiefidedmemchecahnainmissmosf

cohfecmhiecmalicsaylnsthyenstihnsaisnoncaenlloucleolslue;lo(as)ea;c(iad)-baacsided-
 bcahseedmicchaelmniocdal-

imficoadtiifiocna;t(ibo)no;x(bid)aoixoidnabtiaosnedbacsheedmchicreamlimicoadlimfocadtiifiocna.tion. Table

4. The influence of chemical functionalization on morphological nanocellulose. Table 4. The influence of
 chemical functionalization on morphological nanocellulose. Surface Methods Reagents AAidiedded

Reagents OPapreamateitoenr SCoeulrLucSCelooseulsorluecfelosssoef

MTeecchhnaMinTqieecuccahhelainqiYucaieild (%Y(i))%eMI)dor(pnhmMo)loor(pgnhmyo)loCgyl%

CZI%et)aPPo(ZotmeetnVteatn)iatlial (SDCmuehmnmfrsoagicle/eyg) H2 SO4 - 5603°C;26S004m50in°

C; PMeieclrsocrystalline Ultrasonication - -46.1 H2SO4 - 63 Hm2SinO4 MicroCrCyesiltuallo-se 30%L:

1N03C-L1C:7253N0.;5CWC: 16 - -46.1 - 58.1 NCC - NCLC:103-1737.57.96

552%2%h62H0Smo2Si4nO504 ° CP;assioPhasFsPiroeunellFstrUuitltrasoUnlitraaastioinnication58.1 77.96

-25 -25 CsluSIOfHo3nH2aSt(OiPoon4s)/tH-Cl - - 2COIS(O33:1H:6in);5U0lm-LMicroScurlyfasteadl-NCC

Mineral trDaMsoFn;RicT;520h line Cellulose Ultrasonication - 79.31(D:10L-:115820;W: 22.7-; 88% --66.1 h:

5.0 Acids nm) H2SO4/HCl - - H2SO4-:HCl:H2OFilteMriPraopcreyrstalline - - - W: 22S-CNC 85 - (3:1:6);

Ultrasonic Cellulose Ultrasonication (D:10-180 nm) - - H2S5O0h4:ZH;1C0l:hH S-CNCNCC - 50 °C; 9-0 min

line CeFillutelroPsaepUerltrasonication 30% - - L:250; W:WN1C:62C2 85 - NCC

C73l.Sh9-%OZC3;H;H19300PimOnhi4n5;0100 - Filter Paper Blending 76-80 NCC (15 min) NCLC:316; W:

31; 81 - ClSO3H H3(PP0o4st-sul- - - L:152; WN:CC 88% 83 -6-62.17 fonation)

m11L00.0D7-MMC;HF3;03PRmOTi4n;;Sulfated NCC Ultrasonication 79.31 2 h 22.7; h: 5.0 -

731.090%-CH;33P00mi4n; 10.7 M H3PO4; Cellulose CNF L: 2500 nm 81 -23 Mineral Acids - - 100 °C; 90

FilterBPiRoatepesteihdraoneol BlendHio(n1mg0otgimenez)er7r6-80 H3PO4 in

1105.07m-MC;nH303PmOi4n; (15 min) L:31N6;CWCL: N3611C0;Cnm 81 83 --34 molten Urea - 10.7 M

CNF L: 330-480 nm 86 -24 2.5 MH3HPCOI;41:05 °C; HCHI3PO4 -- Blending 1004°0Cm;i3n0 Filter Paper

(40 min) - NCC NCC 83 W: 20 79% -2-7 (mmol/g) - - -SO3 H - (0.0985) -SO3H (0.0-985) -OS.O403-9H -

PO3 (0.0108) -SPOO33H (0.04.345029) -PO3 (0.018) -PO3 ((01-P-.00O31380)8) -PO3 (1.173) -PO3 (0.4-

352) Ref. [29] [29] [134] [134] [135] [135] [136] [[113376]] [135] [137] [138] [135] [135] H2 SO4 Acetic Acid

HC-l 6M HCl FormHic3APcOid4 in 0.015 M - molten FeCl3 Organic Acids Lactic Acid HCl Urea - min

1800.7°C;3 h H3PO4; 101005°C; 390h 8m0-iCn; 4 h 10.7 M H903P-CO;46; h 150 °C; 30 15m0-inC; 3 h

Bleached eucalyptus - kraft pulp CteethllaunloosleCRBoetistooi-n- Ho(1m0otgimenBe(2ilsez0)nemdrinng)

Mduicerocrystalline Cellulose Bleached eucalyptus kraft pulp Cotton 81 NCC L: 264; W: 16 30 L:

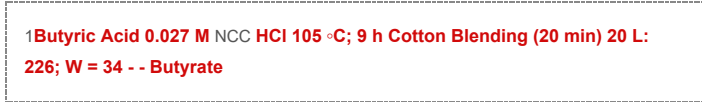
2C5N0LOF:n26Nm9C;WC: 4581 - - NCC NCLC:236; W: 25 Blending (20 min) - nLm:200; W = 20 L: 610

nNCC 83 - 75 CNF L:594 L: 330-48N0CC 86 80 -33 - -23- 88 -1.7 -34 75 -6.53 80 -24 - -SO3 H

(0.015) -PO3 [139] (0.-018) [[114308]] Formate (-OP.4O)3 [141] (1.038) Formate [142] -PO3 L(a1c.t1a7te3)

[143] Table 4. Cont. Methods Reagents Aided Operation Sources of Reagents Parameter Cellulose

Mechanical Technique



[140] -

170% MA; 100 °C; 45 min Bleached eucalyptus - **12% NCC - -33 -COOH**

[144] kraft pulp (0.29) Maleic Acid (MA) - 60% MA; 120 °C; Bleached Microfluidizer 3%

1L: 329.9; h = 15.9 - -46.9 -COOH

eucalyptus (0.368) 2 h kraft pulp (120 mPa; 5 -COOH [145] passes) 84% CNF h: 13.4 - -45.2 (0.059)

1Oxalic Acid (OA) 8.75% OA; 110 °C; NCC - 15 min Filter paper Sonication (60 min) 93.77 L: 150-200; - -36 -COOH, [146] W: 5-20

0.29 - 70%

1OA; 100 °C; 1 h Bleached eucalyptus - **24.7 NCC 80 -42.5 -COOH**

[144] kraft pulp -

130% OA; 100° C; Sonication 30 min Celery

(

118 min) 76.8 CNF h: 5.5 49 -32.9 -COOH

[147] - 5% - -COOH Malonic Acid 80% wt of 0.025 M Malonic Acid; 140 HCl °C; 3 h

119.8% 75 - -COOH - 3.4% - - Malic acid

A80c%id;w14t0of-MC;a3lihc Ramie Blending NCC -COOH, (1.617) 0.05 M Cellulose (5 min) L: ~220; W: ~12 [148] HCl 20% 78 - -COOH - 5.1 - -COOH 0.05 M 80% wt of Citric HCl Acid; 140 °C; 3 h 20.5

178 - -COOH, (1.884) Citric Acid - NCC, -COOH

, 80% wt of Citric Bleached 32 L: 251; W: 21 78 -122.9 0.65 - Acid;

1100 °C; 4 h Baggase **Pulp Ultrasonication**

-

1CNF, L: 654; W: 32 69 190.3 -COOH

, [149] 0.3 TEMPO (0.094 mmol)-NaBr (1.57 - mmol)- NaClO (1.24 M); 10 °C; 45 min Nanocrystalline NCC, Cellulose Ultrasonication - L: 100; W: 5-20 80% - - [150] TEMPO/NaCl TEMPO (0.1 /NaBr mmol mmol)- NaBr (1 mmol)- NaClO (5 -COOH; - HBKP mmol/g Ultrasonication - CNF 85% - -CHO cellulose); (1.191) [151] Oxidation Ambient Treat- condition; 1.5 h ment 50 mM TEMPO, 5 -COOH; TEMPO/O₂ /Laccase U mL⁻¹ laccase; HBKP Ultrasonication - CNF, L: > 100; W: 4-8 - -CHO 96 h (0.837) Sequential Periodate-Chlorite Oxidation (1). 46 mmol 1 M NaIO₄; 50 °C; 4.5 Acetic h followed by (2). Acid (2) 12 g NaClO₂ 50 °C; 40 h Hardwood Pulp Homogenizer (5 passes; 80 MPa) - CNF, L: 95.8; W: 2.72 - -128 -COOH (2.0) [152] - COOH APS Oxidation - 1 M APS; 75 °C; Cotton Linters - 34.4 CNF, (0.16); 16 h L: 95.8; W: 2.72 63.8 - -SO₃ [153] (0.98) In general, NCC isolation comprises exposing pure cellulose material under strong acid hydrolysis with strictly controlled operating parameters such as temperature, agita- tion, time, and concentration of chemical species. As mentioned earlier, various chemical reagents such as H₂SO₄, HCl, HBr, and H₃PO₄ have been utilized as cellulosic disinte- grators. The selection of acid reagents has the most crucial role in determining drug carrier characteristics and synthesis pathways for incorporation or grafting through chemi- cal/physical modification for particular functional groups. The amorphous decomposition using HCl and HBr is not widely adopted because they provide low dispersion stabil- ity of NCC and increase the agglomeration tendency of NCC in an aqueous suspension. H₂SO₄ and H₃PO₄, on the other hand, exhibit better performance as a hydrolyzing agent because the chemical moieties can be attached to the hydroxyl group of NCC during the reaction to isolate charged surface of NCC for subsequent incorporation of phosphate or sulfate functional groups. The new functional group incorporation causes the spontaneous dispersibility of NCCs in an aqueous environment due to the colloidal stability restora- tion through electrostatic repulsion refinement, which is the preferred characteristic of drug carriers. A subsequent treatment of H₂SO₄ followed by HCl synthesis

30has been utilized to control the sulfate moieties on the NC surfaces

. The as-synthesized particle had a similar

7particle size to those particles directly acquired from acid hydrolysis.
Nevertheless, the surface charge density can be

adjusted on the hydroxyl groups exploited by sulfate groups [49]. Lin and Dufresne [137] proposed a strategy of inaugurating progressive sulfate group content on NCCs surface through the modulation ratio of reactants and post-sulfonation (chlorosulfonic acid) and desulfonation conditions. They also evaluated the impact of sulfonation degree on the morphology, dimension, physical characteristic, and surface chemistry of modified NCCs. Diverse zeta potential ranged from -7 mV to -66 mV and approximately 0.0563 mmol/g– 1.554 mol/g of sulfonation degree was acquired. Therefore, it is indicated that the zeta potential of nanocellulose is mainly controlled by the sulfonation degree of nanocellulose itself [137]. Wijaya et al. [29] successfully isolated NCC through sulfuric acid hydrolysis of bleached passionfruit peels waste fiber by adjusting the acid concentration, hydrolysis time, and reaction temperature. The NCC was used for tetracycline hydrochloride adsorption through electrostatic and Van der Waals interaction. The adsorption isotherm was correlated using Langmuir and Freundlich isotherm models. With pH environment adjustment, the adsorption affinity of the drug can be altered to control the uptake and sustained release of drugs [29]. (2,

142,6,6-tetramethylpiperidine-1-oxyl)-mediated (or TEMPO-mediated)
oxidation of nanocellulose has

arisen as an alternative NC isolation route to replace the conventional acid hydrolysis method due to its environmentally friendly and facile synthesis nature. The synthesis starts by using TEMPO/NaBr/NaClO or TEMPO/NaClO₂/NaClO as a reagent. TEMPO (stable nitroxyl radical) forms as the catalyst for NC synthesis, which further transforms into N-oxoammonium salt ($R_1R_2N^+=O$) under certain conditions while the NaClO acts as a primary oxidant [46]. Both NaClO and NaBr can reversibly transform the N-oxoammonium salt into TEMPO form. The hydroxymethyl groups of NC (primary hydroxyl groups located on C6) are selectively transformed into carboxylated groups while the secondary hydroxyl groups remain unchanged (secondary hydroxyl groups located on C2 and C3) [66]. The incorporated carboxyl groups imparted negative surface charges from the change in the environment pH, which leads to improved colloidal stability. As reported by Montanari et al. [154], TEMPO-mediated oxidation with the degree of oxidation 0.24 has imparted negative charges on the crystalline regions of nanocellulose, which provide dispersibility and individualization improvement time decreasing the crystallite size [154]. Meanwhile, Habibi et al. [150] underlined that the TEMPO-mediated oxidation did not affect the morphological and crystallinity of NCCs. Furthermore, they highlighted that the ratio of primary oxidizing agents affected the negative charge of NCCs [150]. A novel oxidation system of TEMPO/laccase/O₂ has been utilized to modify NC. The TEMPO/laccase/O₂ system with sufficient catalytic amounts of laccase and TEMPO reagent produced

12reactive TEMPO+, which subsequently transformed primary hydroxyl moieties
into aldehyde

moieties through oxidation. After the oxidation, the reactive TEMPO+ was reduced into N-hydroxyl TEMPO. However, no-cycle regeneration occurred between

12TEMPO+ and N-hydroxyl TEMPO due to the

breakdown of the

12primary hydroxyl groups of polysaccharides and laccase molecules

. Furthermore, the

12N-hydroxyl-TEMPO was accumulated in the reaction

environment due to the absence of active laccase in the system. Therefore, a large amount of TEMPO and laccase and prolonged reaction time are required to oxidize the primary hydroxyl groups, which are considered major disadvantages of this process [151]. TEMPO-mediated oxidation was mainly used to modify NFCs before mechanical defibrillation to promote the fiber's individualization.

35TEMPO-mediated oxidation leads to the breakage of the

strong intra-fiber hydrogen coordination to facilitate the softening and impairing of its rigid structure, which is beneficial in converting TEMPO-oxidized cellulose fiber into highly crystalline individual nanofibers through mechanical treatment. The NaClO concentration and mechanical treatment strength were considered crucial

factors in determining the polymerization degree, carboxylate group numbers, and CNFs yield. Carlsson et al. [155] emphasized the influence of surface charges in nanocellulose formulation as a drug carrier by introducing TEMPO-mediated oxidation in mesoporous cladophora cellulose for aspirin degradation. The surface charge negativity (

27 **carboxylate content $0.44 \pm 0.01 \text{ mmol g}^{-1}$** significantly accelerated the

degradation of aspirin compared to the native source of CNFs, which had a deficient

27 **surface charge ($0.06 \pm 0.01 \text{ mmol g}^{-1}$). This**

phenomenon is caused by the strong interaction of opposite charge entities between aspirin and TEMPO-oxidized cellulose nanofibers (TOCNFs), leading to increased partial amorphization ability inside the mesoporous TOCNFs [155]. Without a chlorine-containing oxidant, 1.1 mmol g^{-1} of carboxyl groups were incorporated onto wood cellulose. High in carboxylate content, wood cellulose underwent tremendous depolymerization during oxidation. In addition, a long reaction duration of up to 15 h was required to achieve

120.6 **mmol g^{-1} carboxylate content**, while 1.1 mmol g^{-1}

was achieved by increasing the reaction time up to 20 h. Prolonged reaction time is considered the major disadvantage of this process. This method has been utilized for nanocellulose modification in drug delivery applications [156]. The sequential periodate-chlorine oxidation selectively and simultaneously incorporates two carboxyl groups through the oxidative transformation of two vicinal secondary hydroxyl groups (located in C2 and C3 instead of C6 position), enabling higher surface charge density introduction. The increase of surface charge density is essential in retaining the colloidal stability of drug carrier and improving the electrostatic interaction between drug and carrier, which increase the loading uptake of drugs. Plappert et al. [152] investigated the pretreatment effect of sequential chlorite periodic oxidation on open-porous anisotropic CNF hydrogel membrane assembly. Hydrogel membranes were used for transdermal drug delivery systems for nonsteroidal anti-inflammatory drugs (NSAIDs) and piroxicam (PRX). By tuning the surface charge density and the amount of carboxylated groups ($0.74\text{--}2.00 \text{ mmol g}^{-1}$) by varying the reagent concentration, the drug carrier uptake capacity can be increased to within the range of

28 **$30\text{--}60 \text{ mg g}^{-1}$ with the surface charge**

-66 mV to -128 mV . The electrostatic interaction

28 **between the cationic drug (PCX) and the anionic** characterized **surface of** CNF membranes is **the**

main driving factor behind the loading of drugs in the membrane [152]. 5.3. Functionalization through Post Chemical Modification via Covalent and Physical Bonding Strategy Maintaining the structural integrity of nanocellulose to prevent the polymorphic transformation and maintaining the crystalline area while modifying its surface are considered the main challenges. Therefore, several post-chemical

11 **modifications have been studied for surface modification and functionalization of nanocellulose** surfaces before **the**

drug upload. Sulfonation treatment is the most common strategy to introduce sulfate groups into hydroxyl moieties of nanocellulose, which produces a highly negatively charged surface. Nevertheless, the degree of sulfonation was highly determined by several factors such as temperature, acid concentration, and hydrolysis time. Treatment of NC with sulfuric acid or sulfonation followed by acid hydrolysis [137,157] can improve the characteristics of NCs. However, these improvements may lead to lowering the colloidal stability of NC due to the reduction in the sulfonate degree. Since the primary goal of the drug delivery system is to achieve higher colloidal stability and strong electronegativity for further electrostatic drug adsorption or modification, straight H_2SO_4 hydrolysis remains the primary treatment for NC modification. On account of the simple and straightforward treatment,

7 **modification of hydroxyl groups at the NC surface** by Fischer **esterification is**

another common approach. Several reactants have been used to acetylate the surface of nanocellulose, such as acetic, citric, malonic, and malic acid with the combination of HCl or H_2SO_4 . The utilization of H_3PO_4 provides NC modification with higher thermal stability than sulfonated NC. Camarero Espinosa et al. [135] suggested that only one hydroxyl group was incorporated by one ester bond of phosphoric groups. Another study by Kokol et al. [138] revealed the possibility of phosphate-modified nanocellulose (P-NC) originating from two structural isomers, either of which can behave as monobasic acid or dibasic groups. Acetylation of hydroxyl groups of NC can also be performed using enzymatic modification. In an environmentally friendly approach, enzymatic modification serves as a favorable modification route without the need for any addition of chemicals and has low energy requirements, improving biocompatibility and

lowering the cytotoxicity of NC for drug delivery. The acid hydrolysis and oxidation treatments are mainly considered as a primary synthesis of nanocellulose. Indeed, during acid-based hydrolysis or TEMPO-oxidation, hydroxyl groups of nanocellulose grafted by anionic sulfate ester groups (-OSO₃⁻) and carboxylate groups (-COOH) produce the negative electrostatic layer of nanocellulose. Consequently, high stability of nanocellulose occurs in the aqueous solution resulting in electrostatic repulsion between individual particles. Maintaining the structural integrity of nanocellulose to prevent the polymorphic transformation and maintaining the crystalline area while modifying its surface are considered the main challenges. Several post-chemical modifications have been studied for surface modification and functionalization of nanocellulose surfaces before the drug upload. Silylation is another approach to modify the surface nanocellulose by conjugating small molecules.

7A series of alkyl dimethyl-dimethylchlorosilane (alkyl-DMSiCl) with various alkyl groups such as isopropyl, N-butyl, N-octyl, and N-dodecyl can be grafted on the surface of NCC in the presence of

toluene. However, the high price and high toxicity of the reagents limit the progress of silylation modification in the drug delivery field. Recently, Li et al. [158] developed an NC template for mesoporous hollow silica material (R-nCHMSNs) for ibuprofen and lysozyme drug delivery. The presence of NC as a template increases the content of geminal silanols on the R-nCHMSNs surface. Nanoparticles with high content of geminal silanols present outstanding delivery characteristics for various drugs [158]. The amine derivatives can covalently bond the surface of NC through a carbodiimide amidation reaction. The majority of

14amidation-mediated couplings were incorporated on the carboxylic groups of pre-oxidized

NC without re-molding the morphology and crystalline native structure. N-ethyl-N-(3-dimethylaminopropyl) carbodiimide hydrochloride (EDAC) has been widely used for the amidation among carbodiimide derivatives. The addition of

20n-hydroxysuccinimide (NHS) is required to avoid

unstable intermediate O-acyl urea formation and to achieve the direct formation of the stable N-acyl urea. The amidation approach was presented by Akhlagi et al. [159] to create a drug delivery system based on chitosan oligosaccharides (CSOS) and TEMPO-oxidized NCC. The carboxylic moieties on the oxidized NCC were coordinated into the primary alcohol and amino moieties of CSOS. Several limiting factors such as medium reaction, time reaction, pH, and the molar ratio of reagent and cross-linker reaction can be altered, translating to the modified grafting behavior and degree of substitution of CSOS into oxidized NCC. Electrostatic interactions were performed to achieve 21.5% of binding efficiency loading and 14% w/w of procaine hydrochloride (PrHy) loading. The rapid release profile observed in this study is suitable for local drug delivery by the oral system [159]. Direct covalent drug attachment towards the NC crystal backbone via a novel spacer arm through amine-mediated couplings is another potential strategy [160]. Tortorella et al. [160] modified NCC via periodate-oxidation-generated NCC-DAC (dialdehyde cellulose) and inserted them into molecules of γ -aminobutyric acid (GABA) via the Schiff base condensation reaction. Subsequently, the nucleophilic substitution of 4-hydroxy benzyl alcohol (HBA) occurred and was followed by an acylation reaction with 4-nitrophenylchloroformate that exerted a carbonate group for nucleophilic substitution of amino contained doxorubicin as model drug nucleophilic. Carbamate linkage adjacent to the linker presents highly stable conditions in an aqueous environment with harsh Polymers 2021, 13, x conditions, either basic or acidic. The drug release of active drugs was achieved α -naphthyl-1-hydrolysis in cells utilizing suitable enzymes to cleave a carbamate linkage (Figure 7). Figure

77...llullstursattriavteivreepreepserensteanltoantioonfcoofnjucognajtuwedgadtodxodrobuoxiocriunboincitno NonCtCosNthCroCusghthcrohuemghicacalhbeomnidcainlgb(otnhidsinpigct(uthreisisprie--tdurraewins frreo-mdrTawornotofrreollmaeTtoarl.to[1r6el0]a. Ceotpayl.ri[g1h6t0]©. SCporipnygreirgFhatc@hmSepdriennegeWriFesabchadmeendGiemnbWHI)e.sAbbadbreenviGatmiobnHs;)N.CACbbsr=ecveilaltuionlsse: NnaCnCocsr=yscteallsu, lDosAeCna=ncoecllruylsotsaelsd,iDalAdeChy=dcee,lGluAlOBSAed=ica-ladmehinyodeb,uGtyAriBcAac=idc,-HamBAin=o4b-uhtydrircocaycibde,nHzyBIAal=co4h-ohly,EdDroCxyHbCeln=zy1-l aeptychroyihdl-oi3nl-.e(3,E-NDdPiCmChE=tCh4yl-nl=aimt1r-oienpthophyperin-o3yp-l(yc3lh-)dlcoiamrrobefoothdrmyiilmaamtied,iendohlpPyrEdoArpoc=hl)Nloc,Nraidr-dbeoi,iNdsoiHipmrSoi=dpeNyl-h-hNyyd-dertrohocyxhlylaosmruiidnceei,n,aiMnmHhid.SeD,=MDNMF- =AhayPnd=hry4od-xdyriomusuestcdhcyimlnlaiemthiidynelo-, DfoMrmAaPm=id4e-.dDimOeXthOyNlaHm2in=odpoxroirduinbiec,iNn,P*Cis=re4p-netiitriovpehmenoynlcmhelormofoolremcualtees,.DIPEA = N,N-diisopropyl-N-ethylamine, anh. DMF = anhydrous dimethylformamide, DOXONH2 = doxorubicin, * is repetitive monomer molecules. 5.4. Polymer Grafting Modified Nanocellulose 5.4. PPoolylymmereGr-rgarfatifntegdMNOcdfiheadsNbeanenocienllurloedseuced as the sought-after functionalization strat-egy toPorleyfmineert-hgeradftreudgNdCelihaesrybeepenfionrtrmodanuccee.dDaisfftehreesnotutegchht-naifqteurefsuhnacvtieobneaelinzadteiovnelsootraetdegtyo itnotroedfianceethfuendctriugnadlegirvoeypspoenrffoorNmCanccoe.alDeniffleyr,ein.et.t,e(c)i)hTnhiquileeshearveeacbtieoen; (die)vOelxoipmeedteo-aincctiirond;u(cieii)fuMniccthoanelaladgdroituiopns;oanntdo (NivC) icmovinaeleannltdy, hiy.ed.,ra(iz)OTnheiosylenntheerseias.ctTiohne;se(iir)eaOcxitiomnes hreaavcetiboene;n(iwii)eMII- idcehvaeelloapdedditfoomp;oalnym(eivr)fuimncintieonaandizhatyiodnrafzoorndersuygndtheelisviesr.yThysesstemreas.ctions haveblneteeegnwaterinllg- dpeovleylmpoepdofnotrothoelyNmCersfuumfactieoncaanzlibaetipoenrformdreudgbdyethlvee'rgyrsayftsitnegmosn.t'

reraecatitino.nF.oFroreexammppele.,KKhhinineeett aall. [[113322]]
 ddeemmoonssttraateedpphhooto--inindduuceedd“c“lilcic“k”chcehmemistisrytfor
 fo(rT(ETMEMPOP)O-o)x-
 oidxiizdeizdeCdNCFNbFeabreianrgincagrcbaorxbyolxicyallicadacmidoimetoieiset(iTeOs(CTNOsC)Nmso)dmifioeddfwiedthwihethihttreile
 niitmilieinim-minede-imateedditaeatterdaztoetleraznodleerunuditerarvuiotreatv(iUolVet)
 i(rUraVd)jiairtriaodni.aTtihoenp.Trehseenpcreesoefnlcueoorfesflcueon-ce
 recschearnaccetechrisatraccaetlriioswticesadfallorlwdierdecftomrodrietoctrimngoonfitNorCintghroofuNghCotuhtrtohuegchaonucterthceelcls'a'nicnecruct
 inlcnbadatdioitnio.nln, daodxdoitriubni,cdinoxaasraubdircuing
 amsoadderlucganmboedaettlcaachnebdevaitataecheedtrovsitaetilcecitrtoesrtaacticioinn-to
 terinatrcioinductoeixntersosdnuecgeaetixvceescshanreggeaotinvteo
 ccahrabrogxeyolngtrtoocpasrbinoxthyle gporolyumpseriinc-gthraeftpeodlyNmCe[r1c3-2].
 graftedUNnCde[s1i3ra2b].le reduction in surface grafting density is nonetheless observed as the
 maUjonrdliemsirtaabtlioenre.dTuhcteisnteirnicsubrafracieergcaafntinhjinddeensittihyeisonpotinmeuthmelegsrsaofbinsegrvthedroausghhoeumtath-
 e jorrelaimctiioantiboenc.aTuhsee
 tshteeriacybearrifearctacnhdinpdoolrytmheerocpovimeruemdtghreaaftvinaiglatbhreouaugtihvoustitthehse.
 Trehaecreiofonre, beacnauasleertheatlviyeerstorfataetgtaychheads
 pboeelynmperrocovseerde,dctahleleadva'gilraabflteingactfirvoemsi't.esU.Tsihnegretfhoirse,maenthalo-d,
 tertheatpivoelysmtreartecghyaihnaassbaenenbepgoropwosnedin,csailltuedon'gtrhaeftsinugrrfacoemh'y.UrsoinxgylthgirsomupesthoofdN,Cthevipaoriiny
 g- moerpecnhaningspcoalnymbegirzoawtionnin(RsOituP)onwiltithe
 tshuerfpacreesheyndcerooxfysltgarmonuopussoofcNtoCatveia(Srmin(Og-cot)p2e)naisngan
 poRlyOmPeargizeantio.nA(nRoOthPe)jrwaiptprthoaeacphreisseantcoemofrsatnansfneoruradocioatlatpeo(ISynn(Oercit)a2)tiaosna(nARTORPP)awgei
 Abnorothmeoriaspobpurotyarcyhlbroamtoimdetr(aBnlBsfBe)r
 arasdthicealApToRlyPmagereinzta.tTiohne(sAeTstRaPnd)wariditha2p-pbrrooamchoeissofbourtdyrru-g
 yldeberolimveirdyeh(BavlBeBb)eaesntwheelAl-r-TeRvPiewageednte.IsTehwesheerseta[n1d32a]r.d
 approaches for drug delivery have been well-reviewed elsewhere [132]. 5.5. Surfactant Modified
 Nanocellulose 5.5. Surfactant Modified Nanocellulose The adsorption of surfactants represents a promising
 alternative for the chemical modification of NC. Surfactants are classified into cationic, anionic, zwitterionic,
 and non- ionic. The distinct properties of the surfactant manifest through its micelle formulation in the
 aqueous solution, which is highly beneficial in the drug delivery system. The lack of a strong covalent bond
 is considered the significant drawback towards enabling molecule release. Therefore, it is necessary to
 study several factors affecting the interaction of surfactant and NC and their impact on drug uptake and
 release. Tardy et al. [165] reviewed several factors that influence the affinity of NC and the surfactant. This
 study provides some additional information on the affinity of NC and the surfactant on the drug delivery
 system. The opposite charge between the NCC surface and CTAB drove the electrostatic interaction and
 physical adsorption for the NCC surface modified with the surfactant. NCC's negative charge creates a non-
 covalent interaction towards the cationic charge of CTAB, resulting in a strong electrostatic interaction.
 Zainuddin et al. [166] pointed out several factors that mainly involve the interaction between NCC and the
 surfactant, i.e., pH and ionic strength, the CTAB concentration, and the ratio of CTAB to NCC. They high-
 lighted that the CTAB concentration and mass ratio of NCC: CTAB affects the interaction of surfactant-
 modified NCC with curcumin as a hydrophobic drug model. Increasing the CTAB concentration intensifies
 the hydrophobic character of the carrier, which is intensely coordinated with curcumin. However, at a high
 concentration of CTAB, the amount of curcumin attached tends to decrease [166]. Low surfactant
 concentration favors the electrostatic interaction between the monomer CTAB head with the negative charge
 of NCC surface, giving hydrophobic properties. While the CTAB concentration increases progressively, the
 adsorbed monomer of the surfactant tends to restructure and initiate surfactant cluster formation induced by
 hydrophobic coordination between surfactant alkyl chains. The CTAB cluster molecules can be absorbed
 through the NCC surface by hydrophobic interaction. However, the hydrophobic coordina- tion of the
 surfactant and NCC manifested as a weak electrostatic interaction, which easily releases CTAB from NCC
 surfaces through the washing. Moreover, an excessive amount of CTAB concentration over the boundary of
 the surfactant critical micelles concentration (0.93 mM CTAB) might provoke the surfactant micelles
 formation on the NCC surface, which degrades the hydrophobic characters. Only ionic interaction between
 the cationic head of CTAB and anionic sulfate ester groups remains unaffected, which acts as available
 active sites for hydrophobic drug loading (Figure 9). Raghav and Sharma [167] reported the coordination of
 the hydrophobic tail of CTAB in phosphate NCC. They also observed that the surfactant types (CTAB and
 TBAB) influence the capability of modified NCC to bind and release the drug. By observing the structure
 configuration, stearic near the central nitrogen in TBAB-NCC causes the insufficiency of drug binding, which
 exacerbates the coordination and controlled release of the carrier [168]. Putro et al. [25] modified the NCC
 with various

18 types of surfactants such as cationic (CTAB), anionic (sodium dodecyl sulfate),
 and non-ionic

surfactant (Tween 20). Different types of surfactants exhibit distinct interactions towards NCC, which
 influenced the electronegativity of modified NCC itself and the drug adsorption–desorption behavior. The
 presence of salt in the system had a significant influence on the uptake of paclitaxel. Different behavior of
 surfactants due to the salt effect significantly influences the interaction of NCC and drugs. They concluded
 that (1) electrostatic and Van der Waals interactions are the primary mechanism of paclitaxel adsorption
 towards surfactant-modified NCC, which can be enhanced through salt addition; and (2) pH played a
 significant role in the drug adsorption and release of paclitaxel by altering the surface charge of surfactant-
 modified NCC and the electrostatic interaction of hydroxyl ions and paclitaxel in solution. Polymers 2021, 13,
 x 28 of 49 Figuri et al. 2021. hematic representation of the surfactant anadnanocrystalline cellulose
 mechanism and its effect on drug ad- adsorption (t(h)hisisfigruerisersir-se-drawn from Bundjaja
 et al. [26]). Copyright ©2022 002E0I Eselsveirie Br. BV. (V.).
 SurRfaagctahnatsahnadvSehaalrsmoab[e1e6n7]wreidpeolryteudstehdetcoomrdoidniafyticnelolufthtoehsehnadnroopfihbboefricotraploofrClyTAB
 soluinblpehdorsupghaadesNorCpCtio.Tnhpeeyrfaolsromoabnsceer.vTehdethsuatrfahcetasnutrafaatctaacnhtmyepnetso(nciThAeBCaNNfDsTuBrAfaBce)
 vitalentoceovtheerccoampaebvialirtiyousfmlimoditiaftieodnNsoCfCCNtoFb'sincdheamndicarellaenadsephthyesdicraulg.hBayraocbtesreirsvtiicngsdutuhre

modtuifirecactioinfigfourradtriuong,csotenavreycannecaersthystsetceemnstr.aTlHneitprohgyesnicianlTinBteArBac-
 NtioCnCocfatuhseessutrheacintasnutffaincidity
 CNFofmdaryugovbeimcdoinmge,twhehaicghgreexgaactorbnatteensdtehneccyoofrCdiNnFationanodrgcaonnictroollveednrt,etlehausseinocfrtehaesic
 the[s1o6lv8]e.nt's ability to assist CNF modification and adsorption of hydrophobic drugs. The
 presencePoufrthoestuurl.f[2ct5a]nmtsodtreifniedgththnesNthCeCcawtiothnivcaarnioduhsydyrpoepschoofbsiucrcfhacatraancttssersuocfCaNscFa.tAio
 carr(iCerT'AspBh),yasnicioalnaicn(dsocdeiummicadlocdheacryalcsteurlifsttic)s,caanndbneorne-
 fionneidcbsuyrafadcdtianngt a(Tswurefeanct2a0n)t. (DCiNffeFrent filmyapnedsofoasmusr-
 fbaactsaendtsCeNx(Fh).bit distinct interactions towards NCC, which influenced the elec-
 trTohneegsaytnivthieytoicfsmurofadaciftiaendtnCaCnCinidtsueclfeamndemthberadnreucgealldlsoyosriptsbioanse-
 ddeosnorbpiticoonmbeahtaivbiliorl.y,The
 whipchreissecnocnesoidfesraeldianttohxecisysmatemriahlafadoracseiglSn.ifTtchaenretfionrfelu,tehneceanoatnrtahleyuapvtaiiklaebolefpsuarclaitcatxae
 havfeerbeenentbceohnasvidioerreedf
 tsourrefapcltaacnetssydntheettoicthsuersfaalctaenfttescgtisvigennitthiceairnltolywintofxiueicintyc.esFothreininstaenrace,ction
 BunodfjaNjaCeCt
 aaln.d[2d6]ruugtlis.lzTehdenyactounracllusduerdfacthaant(1(r)aerlaescatproosntiant)ceaxntrdacVteadnfdroemrWSAapainlsdiunterraarcatkions
 DCafrreuitthsetopmrmodairfymnaencohcaenlilmslosoefvpiaachlyitadxreolpahdosboicrpintitoenratcotwioanr.dTshseurrefsauctlatsnot-
 frmthoediifisetdudNyCC, indiwcahtiecdh tchaantbtheenrharansaescaepdonthnr-
 omuogdhifisaeldtaNdCdCtioenx;haibnidts(2a)lpoHwepriaaydesdorapstiognnicfiacpanabirtioitlye ionfthe
 tetradcryugliandesroerlpattiivoentaonsdymethheatsicesoufrpfaaccliatnatx-
 embbodyiafiletedriNnCcGCh(eCsTuArfBa,cTewcheaerng2e0,oafnsdurSfaDcSta).nTt-hmeod-
 utliizfaetdioNnCoCnaantudrtahlesuerlefacctrtaonstastfiocirnthteeramcotidoinfioafthioyndroofxnyalnioocneslaunodspeamclaittaerxieallsinresmolaitnio
 challengeS.UOrftahcetarnbitsoahcatviveeaoclosompeoeounwdsidthealytwuseerdeatottamchoeddifytocthelheluslursfeacneanofofNibCeCrfmoraypocoaurts
 limiutebdleindtreurgacatdiosnorfpotriotentrapacrycolrimneamncol.eTcuhleessu.rfactant attachment on the
 CNF surface is vital 5.6.tPooolyveelerctormolyetevsa-Briaosueds Nliamniotcaetilounlosseof CNF's
 chemical and physical characteristics during modification for drug conveyance systems. The physical
 interaction of the surfactant and
 CPNoFlymelaeyctorovleyrteosmareetchheaarggedrepgoaityiomnetresnidnewnchyciohftChNeiFrienpaenatoinggaunnictssocloventati,nththues
 einleccr-eas- troliyntge
 gthreuosopl.vlenpnt,oslaabrisliotyuttoioanssissutCNaFsmwoatdeifr,ictthateisoenpaonldymadesrosrdpitsiooncoiaftheyindtroopcahtoiboicnsdorrugs.
 anioTnhse.Tphreesmenocsetcoofmrthmeonsuarfpapcrtoaanctsttoremnagktheeansfnthnctioacnaatilopnoicyaenledctrohoylydtreocpahroibeircischtoarcarce
 of a multilayer carrier, through electrostatically assembling layer-by-layer (LbL) the nanocel- CNF. A carrier s
 physical and chemical characteristics can be refined by adding a surfac- lulose (either negative or positive
 surface) with an oppositely charged polyelectrolyte. tant (CNF film and foams-based CNF). Currently, the
 development of drug delivery carriers through LbL assembly has drawn The synthetic surfactant can induce
 membrane cell lysis based on biocompatibility, considerable

4attention due to their unique properties. Various physical interactions **such**
 which is considered a toxic material for cells. Therefore, the naturally available surfactants **as**

hydrogen bonding, hydrophobic interaction, and Van der Waals interaction are present in functional polyelectrolyte carriers. Those interactions act as the driving force in drug binding and maintain the stability of the multilayer [169]. LbL hybridization assembly of nanocellulose with other organic and inorganic materials usually instigates an outstanding performance improvement for the entire LbL system to stimuli-responsive and localized drug delivery. Early development of the LbL approaches was demonstrated on the flat substrates and is currently extended to spherical particles. Coating LbL film on a spherical sacrificial template becomes another layer-by-layer assembly approach for hollow polyelectrolytes capsule formation to encapsulate and re- lease the drug. Melamine formaldehyde (MF) is a popular template for microcapsules preparation via LbL assembly due to narrow-sized distribution and optimized disso- lution conditions [170]. The physicochemical characteristics of templates such as size, shape, porosity, colloidal stability, and template solubility modulate the characteristic of as-synthesized hollow capsules. For instance, the capsule size can be adjusted depending on the size of the template, which is common in the range of 150 nm to a few microme- ters [171]. Nanocellulose has been used to construct the interior of multilayer thin film and hollow microcapsules for various types of therapeutic molecules loading such as DNA, RNA, protein, and drugs. Several aspects should be considered to assemble suitable polyelectrolyte complexes through the LbL system, i.e., charge stoichiometry, charge density, molecular weight, poly- electrolytes concentration, pH, ionic strength, order of addition, mixing ratio, and mode of mixing the polyelectrolyte solution. These factors greatly influence the drug carrier thickness, the surface charge, and the morphological structure, such as the size, shape, and porous structure of the drug delivery system. Reviews on some crucial aspects that influence the stability of polyelectrolyte complexes for drug delivery systems are available elsewhere [172]. Mohanta et al. [173] produced an NCC multilayer thin film with counterionic poly- electrolytes (chitosan) on a quartz crystal microbalance (QCM) plate through LbL growth assembly. They also developed hollow microcapsules using MF as a template. By varying the concentration of the polyelectrolyte (either NCC and chitosan) and the number of depositions, a homogeneous multilayer thickness with a porous structure can be obtained. The thin film and microcapsule were utilized as carriers for hydrophilic drugs (doxorubicin) and hydrophobic drugs (curcumin). The protonation of amine groups in acidic conditions becomes the driving force for doxorubicin release, while the concentration difference be- tween the medium and carrier is considered the primary factor affecting curcumin release. The stimulus-responsive pH in LbL system-based nanocellulose may apply to local drug transport and tumor therapy [173]. Other types of layer- by-layer assembly approaches were also used to construct PEC-based nanocellulose by incorporating various types of polyelectrolytes. For in- stance, Li et al. [174] proposed the buildup technique of LbL for opposite-charge building blocks (e.g., cellulose nanocrystal (NCC), polyethyleneimine (PEI), cis-aconityl- doxorubicin (CAD), and building blocks of folate (FA)). The highly negative charge of NCC serves as an anchor to carry the positive-charge PEI through electrostatic interaction as an intermediary layer. The coordination of NCC-PEI resulted in positive-charge material for electrostatic adsorption of the negative charge of FA and CAD to construct the outermost layer, which took place sequentially (denoted as FA/CAD@PEI@NCC). The presence of FA on the surface carrier increased the active targeting ability

towards folate receptors in the tumor cell. Cis-aconityl amide linkage in doxorubicin (CAD) can specifically release DOX at the lysosomal pH due to the pH labile characteristic and hydrolysis cis-aconityl amide linkage by β -carboxylic acid under low pH. The integration of each layer can increase the uptake to 20 times larger than its counterpart due to the strong electrostatic charge. Besides the surface chemistry carrier, the carrier's morphological structure also helps the carrier delivery reach tumor cells [174]. Another potential form of polyelectrolytes, including hydrogel, aerogel, lightweight porous materials, and integrated inorganic-organic composites, are thoroughly discussed in the following sections. 6. Hydrogel Based Nanocellulose for Drug Delivery

4 Hydrogels are three-dimensional (3D) cross-linked polymeric networks that

carry absorbed water and store a large quantity of water in the swelling state. The hydrogels can be cross-linked through physical (non-covalent interaction), chemical (covalent coordination), or an integration of both physical and chemical cross-links [175]. Given its biocompatibility and stimulus-responsive swelling behavior, the hydrogel has gained attention for drug delivery application. As a drug carrier the physically cross-linked hydrogel is preferable to the chemically cross-linked hydrogel. The covalently cross-linked hydrogel generates a permanent structure that limits the swelling ability, and therefore, most chemically cross-linked hydrogels are used as implantables. Furthermore, the incorporation of the drug via adsorption towards chemically cross-linked hydrogel restrains the loading efficacy. Although the cross-linked reaction may perform drug conjugation on the hydrogel, it sacrifices the chemical integrity of the drugs. Therefore, it is more desirable to construct a hydrogel delivery system where simultaneous gel formation and drug adsorption can occur in an aqueous environment without covalent cross-linking. Due to the presence of sol-gel transition characteristics (such as swelling behavior, mechanical strength, and network structure), which are affected by the external stimulus such as pH, thermal, light wavelength, ultrasonic waves, pressure, magnetic field, and electrical field; the smart hydrogel-based nanocellulose has been well-developed for various drug delivery formulation. Diverse types of polyelectrolytes can modify the substantial charge of nanocellulose (either positive and negative) to form a variety of intelligent hydrogels such as injectable hydrogel [161], stimuli-responsive hydrogel [176], double-membrane hydrogel [177], supramolecular hydrogel [178], microsphere hydrogels, bacteria cellulose hydrogel [179], shape memory-based bacteria cellulose [180], and aerogel/cryogel [174]. All those hydrogels have desirable physical and chemical characteristics to be adapted to various drug delivery systems. Liu et al. [161] reviewed the current development of nanocellulose-based hydrogel and its modification for drug delivery systems. However, double-membrane hydrogel and supramolecular hydrogel are excluded from their review [161]. Different types of hydrogels have diverse morphological structures, network coordination, and functional groups, affecting the drug's diffusional path during adsorption and release. Double-membrane hydrogel was developed by Lin et al. [177], consisting of an external membrane composed of alginate and consolidation of cationic NCC (CNCC). Two different drugs were introduced on different layers of the membrane with contrasting types of release behavior. The outer hydrogel releases the drug rapidly, while sustained drug release occurs in the inner membrane hydrogel. This phenomenon occurred due

6 to the 'nano-obstruction effect' and 'nano-locking effect' induced by CNCC components in the

hydrogels. The 'nano-obstruction effect' offers sustained drug release throughout fragmentary disintegration, and the 'Nano-locking effect' is responsible for restricting the burst of drug release through progressive hydrogel disintegration (Figure 10). The different compositions and properties of external and internal hydrogels affect the drug's behavior and diffusional path [177]. sustained drug release occurs in the inner membrane hydrogel. This phenomenon occurred due

6 to the 'nano-obstruction effect' and 'nano-locking effect' induced by CNCC components in the

hydrogels. The 'nano-obstruction effect' offers sustained drug release throughout fragmentary disintegration, and the 'Nano-locking effect' is responsible for restricting the burst of drug release through progressive hydrogel disintegration (Figure Polymers 2021, 13, 205120). The different compositions and properties of external and internal hydrogels affect the drug's behavior and diffusional path [177]. (A) (B) Figure 10. (AF)igTuhree r1o0u.t(eAf)aTbhreicaotioutne foafbsriincagtieonmoefmsibnrgalneamenmdbroaunbelaen-medmoubrbraen-mememicbrroasnehmeriecrhoysdprhoegreelhwydithroi-ts optical (this figure isdoreupbrlien-mtedemwbirtahnpeemmicircsossionpnefremohyrderfo.g[1e717](t.hiCsofipgyurrieghist r@ep2r0i1n6teAdmweithricpanerCmhisesmioincaflroSmocireetfy.);:1(7B7)].schematic microscope ogfeslinwgiltelmitesmpobrtiacnael mSAic/rCosNcoCpCemoficrsionsgplehemreemhydrarongeeSIAan/CdNSACC/CmNicCrCosdpohuebreleh-mydemrobgrealnaenmdSicAro/CspNhCerCe hydrogel Copyright © 2016 American Chemical Society); (B) schematic illustration of dual drug release mech- illustration ofandiusaml dffroumg raeldeasuebml-elcahyaenrimsmemfrbormanae dhoyudbrloeg-lealyceormmstermucberadnferohmydCroagtieolnciocnNstCruCctaenddfraolmginCaatteio(nthicisNCC and Alginate (thisfiffiguurereisrereddrarawnnfrformmLLinineettaal.l.[17777]).CCoopyyirrigghtt @22001166AAmmeerircicaannCChheemmiccaallSociety). SupramoleculSaurphryamdrolgeeculslahrvyedboreognelcshhaarvaectbeerieznedchaasrathcteer3i-zDedsoalsidthnee3t-wDosroklidyndertow-ork hydrogel dination, andtocioanti, oann-dtt caantdiotr--ttainndttrra-rtctionntesr.alnciticoonnt.rlanstootntrhaestchoemthieccahlleymircioaslsly-licnrkoessd-hinyk-ed hydrogels, gel organizedobrgyannoizne-dcobvyalneonn-icnotveraalcitoninstesruacchtaiosnshysudcrhogaesnhlyindkroaggeen,hlyindkraogpeh,ohbyidrcroopohr-

obic coordina- drogels, gel
 mgoerpmhoolropghyoilsogeqyuiisiebqrautielidbrthatreodugthhrcoouvgahlecnotvcaoerndtincoatirodni;ntahteiosnu;ptrhaemsoulpecruam-
 olecular hy- lar hydrogel mdroorgpehlomloogryphisoslotagbyiliiszesdtabbyliazendobny-caovnaolnen-
 ctovnatelernactiinotne.rSacutpiornam.Soulepcruamlarolheyc-ular hydrogel drogel has
 beheanssbyenetnhesysintzehdesthizreodugthhroeuxtgehnsxivtee,ndsiivvee,rsdeivseurpsreasmuopreacmuloalreccuolnafriguomafitgounrsa,tions,
 includ- ing host-guest complexation, biomimetic interaction, hydrogen bonding, stereo-complex including
 host-guest complexation, biomimetic interaction, hydrogen bonding, stereo- formation, and ionic and metal-
 ligand. Hydrogel-based supramolecular self-assembly through host-guest complexation is the most widely
 explored method for supramolecular hydrogel formation. Specifically, supramolecular hydrogels constructed
 by host-guest inclusion between polymer and cyclodextrin demonstrated the thixotropic reversibility, which
 is advantageous for syringe drug delivery. Lin and Dufresne et al. [178] produced supramolecular hydrogel
 DDS by self-assembly of a covalently grafted α -cyclodextrin (α -CD) NCC surface with epichlorohydrin as a
 cou- pling agent through a one-step process. Furthermore, pluronic composed of triblock copoly- mers

2with different molecular weights (Pluronic F68 or F108), both bearing hydrophobic

2host-guest inclusion between polymer and cyclodextrin demonstrated the

thixotropic re- versibility, which is advantageous for syringe drug delivery. Lin and Dufresne et al. [178]
 produced supramolecular hydrogel DDS by self-assem- bly of a covalently grafted α -cyclodextrin (α -CD)
 NCC surface with epichlorohydrin as a

2coupling agent through a one-step

process. Furthermore, pluronic composed of trib311oocfk47

2copolymers with different molecular weights (Pluronic F68 or F108), both bearing hydro- phobic poly-(propylene glycol) (PPG) and hydrophilic poly(ethylene glycol) (PEG) seg- ments (PEG-b-PPG-b-PEG

), were immobilized on NCCs via the inclusion interaction be- twp(PoeEelynG--(bph-rePohPpyGydl-erbn-
 epPhEgoGlyb)ci,cowls)eegr(ePmPiemGnm)taoonfbdpiloihzlyeydmroeoimpahNnidClicCcyspcovlloiyad(eethxthetryiinlneccn(IFueisgguiolynreocio1nl1t)e)
 (.rPaTEchtGeio)snusebpggermatwmeeno-tns letchuelahryhdydroprohgoebli-
 cbasseegdmNenCtCofwpaosluymtleizreadnadscaydclroudgecxatrrimie(rFFiogrueant1i-1c)a.nTcheer
 isnupvritarmooorelelecauslear ofhyddorxoogruelb-bicaisne,dwNhiCcCh
 ewxahsibuiltieldizesdusatsaianeddrudgrcuagrriieelrefaosreabnethi-acvainocre(r6i.n5
 vdiatryos).r.eTlehaesekoinfectiocx-
 reolreuabseicmine,cwhhancihsmexfhoilbloitwedstshuest'aobinsetdrudctriugn'realnedas'elobcekhinagv'ioerff(e6c.t5s.dTahyes)y.
 fTohuenkdintheatitsruepleraas-e
 mmoleecchualnairsmhyfdorologwells,thuep'oonbsbtreuincgtiomno'adnifdie'dlowkiiitnghN'eCffCec,tisn.dTuhceeyafopuhnydsitchaaltosbusptraumctoioien
 r
 fehcyt.dMroogerelso,vuepro,nthbeeiangemquoadtiefelodawdiinthgNoCfCN,CinCdugaevaepshtyrosnicgalionbtesrartuctioionn(eef.fge.c.t.hMydorroego
 bothnediandge)qiuinasitdeelosaudpirnagmoofleNcuClaCrghayvderosgtreolsnganidnteenraacbtlieodnt(hee.gp.,ohlyymdreorsgeton
 absosnodciiantge)inintshidee
 trsiduipmaemnsoloencuallaprehrycodraotgineglsnaentdweonrakb,lwedhitchheppoolvymideerssato"laoscskoicnigateeffinectth"ettorridemlayentshieonda
 r-
 sicoonlaotfindgonxeotrwoobricki,nwmhioclhecpurloevsid(Feisguar"elo1c2k).nTgheeffseucts"tationeddelareylethaseeddifefupseinodnsoofndothxorau-
 bCicDin
 comnotelencu,ltelhe(cFhigauinrele1n2)g.tThhoefstuhsetapiinuerdonreicpasoeolydmepeer,nadnsdonththeama-
 oCuDntoonfNenCt,Cthleoaccheadininlensgut-h porafmthoelepluurlaornhicypdorloygmelesr,[1a7n8d].the
 amount of NCC loaded in supramolecular hydrogels [178]. FFIGuurer1111.. Construction pathwayooff(!!)

2cellulose nanocrystal (β)CD-g-CNgraraffetedd β

-cyclodextrin(!!II))cocompplexex inclusion between Pluronic polymersanadd (β)CD-g-CN;(!!III))
 supramolecular hydrogels comprisingananinsitu

2inclusion between (β)CD-g-CN/Pluroniachadnd α -CD(a)a) hydrogel CN-CD/F68

-a2nadnidsitasnadnidsits morphological evidence,(b)

**2b) hydrogel CN- CD/F108-2 andits morphological evidence, (c(c))water, (d)dd)rug-
 loaded hydhyodgreolgCeNi-CD/F108-2-Dox**

. ThisTfhigisurfeigusreepirsintee-d
 pwrnitthedepewmithispsieormfirsofmion[1f7r8o]m.C[1o7p8y]r.igChotp@yr2i0g1h3t
 A@m20e1ri3caAnmCehriecmanicCalhSeomciectayl.Society. Kopac et al. [181] pointed out that the main

parameter for controlling the drug delivery rate in an anionic hydrogel-based nanocellulose is the average pore size (mesh size), controlled by selecting cross-linked and biopolymer concentration along with the adjustment of pH and temperature. The changes in the ionic strength and hydrogen bonding of functional groups in the internal hydrogel structure are responsible for altering the polymeric hydrogel network, which affected the average pore size of hydrogel (Figure 13). Due to the smaller hydrodynamic size of the drug relative to the mesh size, the drug can rapidly diffuse through the hydrogel network and vice versa without a steric barrier. However, both drugs can have a similar

32 drug release rate by modulating the mesh size through cross-linking density and

biopolymer ratio variation [181]. s 2021, 13, x 33 of 49 Figure 12.

ScFhigemuraeti1c2i.lSucshtreamtioantocofilpluosstsriabtieonlocokfipnogsesffibclct

loofctkhiengdreuffgevtiaohfothste-gdruesgt vniaculhuoisotn-ginuessutpirnacmluoslieocnulanr hydrogel

Polymecrso2n0s2t1r,u1c3t,exd

sfurpomramcyocleodcduleaxrthinydarnodgeclhceomnsictraullcytemdofrdioimfiedcyncnaondoexcrtyrisntaallnindeccheelmulicoaslely(tmhosdpificetdurneani

[17348].of 49 Copyright ©c2e0ll1u3loAsem(ethriicsapnicCthueremiiscareldSroacwienty.f)rom [178].

Copyright © 2013 American Chemical Society.) Kopac et al. [181] pointed out that the main parameter for

controlling the drug delivery rate in an anionic hydrogel-based nanocellulose is the average pore size (mesh size), controlled by selecting cross-linked and biopolymer concentration along with the adjustment of pH and temperature. The changes in the ionic strength and hydrogen bonding of functional groups in the internal hydrogel structure are responsible for altering the polymeric hydrogel network, which affected the average pore size of hydrogel (Figure 13). Due to the smaller hydrodynamic size of the drug relative to the mesh size, the drug can rapidly diffuse through the hydrogel network and vice versa without a steric barrier. However, both drugs can have a similar

32 drug release rate by modulating the mesh size through cross-linking density and

biopolymer ratio variation [181]. Figure 13. Schematic illustration of the swelling mechanism of hydrogel

fabricated from TEMPO-mediated CNFs and alginate towards drug release (this figure is redrawn from

[181]. Copyright © 2020 Elsevier B.V.). 7. Lightweight Porous Based Nanocellulose for Drug Delivery

Lightweight porous materials have been classified as a 3-D solid class of material with several features

33 such as high specific surface area, very low density

(<50%), and diverse pore structure with

3 various pore sizes ranging from nanometer to micron

. Sponge, foam, and aerogels

3 are the three major categories of lightweight porous materials

. The 7. Lightweight Porous Based Nanocellulose for Drug Delivery Lightweight porous materials have been classified as a 3-D solid class of material with several features

33 such as high specific surface area, very low density

(<50%), and diverse pore structure with

3 various pore sizes ranging from nanometer to micron

. Sponge, foam, and aerogels

3 are the three major categories of lightweight porous materials. The sponge is constructed by

gas dispersion in the solid matrix, commonly present as an open cell structure of low density porous elastic polymer. The sponge has a macroporous structure full of gaps and channels, permitting easy access to water or molecules flow [182]. Similarly, foam can be made through the steady gas dispersion into a hydrogel or solid matrix and even liquid. Foam is commonly characterized as having a bubble diameter (pore diameter) greater than 50 nm [183]. Aerogel is a three-dimensional (3D) porous material constructed by self-assembly of the colloidal component or polymeric chains, creating nano-porous networks that can be filled up with a gaseous dispersion medium. Aerogel is prepared through the wet-gel drying process by removing the liquid component in the hydrogel, which is replaced by a gas constituent while still preserving the gel network [184]. The specific surface area of aerogel can reach up to 1000 m² g⁻¹ with a porosity

range between 80 and 99.8%. On the other hand, other aerogels, namely xerogel and cryogel, have been prepared by evaporation and freeze-drying. Detailed preparation of light-weight porous material-based nanocellulose has been reviewed elsewhere [185]. For the drug delivery field, carrier morphology, especially the porosity structure, controls the drug adsorption and release since the drug will pass through the internal pore to be retained inside and release outside regardless of the chemistry interaction. Sun et al. [186] underlined that the critical factor in controlling and modulating the pore structure of ultralightweight porous materials is selecting a drying method [186]. Initially,

3freeze-drying, supercritical drying, and evaporation drying

have been utilized in fabricating ultralightweight porous materials. Evaporation drying has emerged as a conventional technique of synthesizing

3nanocellulose-based porous materials. However, there are

several major drawbacks, such as

3internal network structure collapse due to the capillary forces of the solid matrix and the difficulty to

prevent the shrinkage. Therefore,

18freeze-drying and supercritical drying have been used as drying methods

to overcome these drawbacks. Freeze

3drying can retain the porous structure through the sublimation of

liquid into gas.

3It is also possible to cross the solid-gas

interface bypassing the liquid critical point through adjusting the temperature and pressure (supercritical drying). Both methods

3effectively retain the pore structure and refine the

porosity and specific surface area of nanocellulose-based porous materials. Aerogel-, xerogel-, and cryogel-based nanocelluloses are promising materials as the vehicle for a drug delivery system. Before the drying process,

4physical and chemical cross-linking are vital in controlling the

3D network formation and porous material performance. Physical cross-linking is commonly established by weaker

25interactions such as Van der Waals, hydrogen bonding, and electrostatic interaction. In contrast, covalent

cross-linking can create a 3-D robust mechanical framework through the action of covalent coordination and polymerization. Chemical cross-linking exhibits better mechanical stiffness and structural stability compared to physical cross-linking. Muller et al. [180] synthesized water-responsive xerogel to retain its original shape by submerging it in water through moisture utilization as the stimulus. The post-modification of BNC with the different supplementary hydrophilic substances was performed to achieve the re-swelling behavior. Rapid re-swelling behavior can be acquired by supplementary magnesium chloride, glucose, sucrose, and sorbitol with up to 88% maximum rehydration. Their findings of re-swelling modified BNC showed the possibility of developing a carrier with controlled release properties for hydrophilic drug model azorubine in the drug delivery system. Li et al. [174] synthesized two types of nanocellulose/gelatin composite cryogels through

6hydrogen bonding and chemical cross-linking with dialdehyde starch (DAS

) for controlled drug delivery of 5-fluorouracil (5-FU).

6DAS subsequently reacted with both gelatin and CNF to form the chemically cross-linked network. The reaction of **aldehyde groups with the hydroxyl groups of CNFs led to the formation of hemiacetal/acetal types of structures.** Furthermore, **the aldehyde**

group presence effectively integrates

6with the ϵ -amino groups of gelatin to generate a Schiff base

coordination. They found

6that the chemical cross-linking of

Schiff bases and hemiacetal/acetate is crucial to regulate the structural porosity of cryogel composite. Since the porosity and cross-linking degree mainly control drug loading, selecting the chemical cross-linking method is crucial. Moreover, the presence of gelatin hydration capability and reversible hydrolysis characteristic of hemiacetal/acetate, along with its morphological structure, is also responsible for achieving

6controllable and sustained release of 5-FU in

a simulated intestinal environment. In addition, the

4cross-linking degree and the porosity can be tuned by

the composition and ratio of CNF, gelatin, and dialdehyde starch. The addition of CNF increases the drug loading and the cross-linking degree [174]. Figure 14A shows that the improvement of surface roughness and cross-section morphology reduces the pore size of cryogel, leading to an increase in the cryogel resistance against ice crystal growth during freeze-drying, resulting in the smaller pore size, higher specific surface area, and lower density. The smaller pore size leads to better drug loading and releases since the smaller pore structure limits the drug looseness (Figure 14B). (A) (B) Figure 14.

(AF)Sgyunreth1e4s.is(Apa)tShywnathyeasindpmathowrpahyolaongdicmalosrtpruhcotluorgeicoafl sdtirufecrtuenret roaftidoifofefreNnFtCr/atGioeloafinNFRCN/FGCe/lGaetiiantin: (a,b) NGDC1/9; (c,dR)NNFCG/GDelaCtin3/(a7.;b(e),Nf)GNDGCD1C/95/(c5.,dS)uNrfGacDeC(a3-7c.);(ecr,fo)sNs-GseDctCio5n/5(.bS,du,rf)ja;c(eB)at-hce);incrflousen-sceecotifomno(brp,dh,of);o(gBic)athlsetstructure of NFC/GelatiinnfClureynocgeelotfomwoarrpdhsodlrrouggiclaoladtrinugct(ulreefosfdNeF)Can/GderlealteinasCereyffioגיעלntcoyw(arrihgdhstsdriudge)lO(Tah sisidree)parinndted with permission fromele1a7s4eje.fCiofcieyrciygh(ri@gh2t0s1id9eA)m(TehriiscafinguCrheemiriceaplrSinotceidetwy)l.th

30permission from [174]. Copyright © 2019 American Chemical Society). Zhao et al

[187] prepared polyethyleneimine (PEI) grafted to amine-modified CNF Zhao et al. [c1r8o7s]sp-Irinepkeadreduspinyegtlhuylateraledimehinyede(PtEol)fogrrmaftaend atoeraomgeinle(C-mNoFdsi-fPieEdl)C.TNhf success of and cross-linkingkeaduersoinggelflourtmaraatlidoenyhddeepetondfosromnatnhaeaprooglyem(eCrNizaFtsi-oPnEl)of. Tmheethsuyclmesesthoafchryelate (MMA) aerogel formation depends on

3the polymerization of methyl methacrylate (MMA) on the surface of

CNFs, which induced the

3formation of the network between PEI and CNF

. Polyethyleneimine (PEI) carries some

3primary and secondary amine functional groups, which

increase the loading of sodium salicylate (NaSA) to 20 times higher than its counterpart (CNFs-based aerogel). The sustained and controlled release was achieved by the

31on the surface of CNFs, which induced the formation of the network

between PEI and CNF. Polyethyleneimine (PEI) carries some

3primary and secondary amine functional groups, which

increase the loading of sodium salicylate (NaSA) to 20 times higher than its counterpart (CNFs-based aerogel). The sustained and controlled release was achieved by the CNFs-PEI aerogel, which is highly responsive to pH because of the protonation and deprotonation of amine groups in PEI [187]. Chemically cross-linked PEI with TEMPO-mediated BC CNF (abbreviated as PEI-BC) for aspirin, gentamicin, and bovine serum albumin (BSA) carrier has been studied by Chen et al. [156]. The PEI cross-linking induced the morphological changes of BC by increasing the density of interconnected structures and thickening the pore walls, which provide the CNF interpenetrated network with improved mechanical strength [156]. Liang et al. [188] proposed a well-balanced dual responsive polymer (temperature and pH) by modifying branched PEI with N-isopropyl acrylamide (NIPAM), which was further grafted onto CNF through the condensation reaction (abbreviated as CNF-PEI-NIPAM). Remarkably, the pH and temperature of the carrier can alter the hydrophobic and hydrophilic characteristics of CNF-PEI-NIPAM [188]. CNF has been combined with the non-edible surfactant to make air bubble confinement by the Pickering technique, generating stable air bubbles encapsulated in wet-stable foams. Using the unique drying technique, the dry-foams with closed holes (cellular solid material-CSM) were made. Although the three-dimensional closed-hole structure presents a fascinating drug delivery system for the prolonged release of the drug because of confined stable air in the internal foam's structure, such structure may induce an elongated diffusional path of medicine to modify the characteristic drug release. CNFs foam as a drug carrier with the positive buoyancy characteristic was synthesized by Svagan et al. [189]. Positive buoyancy characteristics resulting from the presence of air are retained in the closed cells. These primary characteristics highlight the practicability of CNFs foam as a floating agent for

9gastro retentive drug delivery systems for site-specific drug release

such as intestinal and stomach systems. CNF foams were synthesized by combining the cationic suspension of CNF

9with the consumable surfactant (lauric acid sodium salt) as a foaming

reagent. Subsequently, hydrophilic drug riboflavin was confined in the wet-stable CNFs foam structure and was further dried to acquire dry foam with a close hole structure with up to 50% drug loading (Figure 15A). The CNFs foam offers structural flexibility with different porosity and tortuosity, which can be modified in terms of shape and thickness and can be sliced into different pieces. An increase in the foam thickness leads to a decrease in the riboflavin release rate. In addition, the morphological foam structure showed

9a long and tortuous diffusion path

, prolonging drug diffusion (Figure 15B). Therefore, the

9diffusion coefficient of the drug through the porous foam structure was lower than the diffusivity of

the drug in the film structure [189]. The addition of surfactant is required to synthesize stable dry-foam-based cellulose nanofibers. Lobmann et al. [190] proposed an innovative way to synthesize stable foams by combining cationic CNF and hydrophobic drug indomethacin. Hydrophobic drugs provided a positive molecular interaction by partially covering the hydrophobic side of CNFs, which further changes the surface energy of CNFs. However, the indomethacin loading in the foams was limited to up to 21% of the loaded drug. An excessive amount of drug loading would destabilize and collapse the foam's structure since a higher fraction of free indomethacin and solvent in the solution was present in the air-water interface, which limited the surface-modified CNF aggregation [190]. (Figure 15A). The CNFs foam offers structural flexibility with different porosity and tortuosity, which can be modified in terms of shape and thickness and can be sliced into different pieces. An increase in the foam thickness leads to a decrease in the riboflavin release rate. In addition, the morphological foam structure showed

9a long and tortuous diffusion path

, prolonging drug diffusion (Figure 15B). Therefore, the

9diffusion coefficient of the drug through the porous foam structure was lower than the diffusivity of

the drug in the film structure [189]. (A) (B) Figure 15. (A). Preparation route of CNF-based foams and its morphological, structural characteristic: (a): CNF-based foams cross-section morphological image; (b) cell structure image of CNF/LA loaded with riboflavin (the arrow points to riboflavin). (B) elongated diffusional pathways of the drug in foam-based CNFs (this figure is redrawn from Svagan et al. [189]. Copyright © 2016

Elsevier B.V.). Svagan et al. [191] performed similar assembling of controlled-release CNFs foam with buoyance characteristics utilizing the poorly soluble drug furosemide as a foaming agent. They highlighted several factors such as the amount of drug loading, the foam piece dimension,

10 and the solid-state of the incorporated drug that influenced the kinetic release

of the drugs. Regarding the solid-state of the drug within the closed cell of foam, at 21% furosemide loading in foam, furosemide mainly exists in an amorphous state of furosemide salt, which leads to rapid release with the increase of the drug loading. In addition, the mass of incorporated drugs inside the foam structure can provide different foam dimensions, which alter the drug release kinetics. Bannow et al. [192] investigated

9 the influence of processing parameters on the foaming characteristic and structure of

nanof foam CNF/indomethacin. They found that the nanof foam density and the number of entrapped air bubbles depend on the pH, the mass of confined drugs, and the preparation route (pre- or post-adjustment of pH) [192]. The development of sponge-based nanocellulose for the drug delivery system by adding citric acid (CA) as a co-cross-linker between branched polyethyleneimine (bPEI) and TOCNFs was conducted by Fiorati and coworkers [193]. CA was added as an auxiliary carboxyl moieties source to improve the cross-linking process to bPEI. They investigated the as-synthesized sponge capability as a drug vehicle for amoxicillin and ibuprofen. The confined drug in the sponge structure with non-contained citric acid moieties exhibited a higher drug release percentage than that with the cross-linker. The presence of citric acid progressively increased the ibuprofen adsorption, while no significant effect was observed for amoxicillin adsorption. The presence of citric acid provided an additional carboxylic group, which was actively involved in the particular interaction with the ibupro- Polymers 2021, 13, x fen molecules. In addition, the existence of CA also refined the mechanical strength and chemical stability of the material through the occurrence of amide bond format3i9onof b4e9tween the primary amines of bPEI and with carboxylic groups of TOCNFs and CA (Figure 16). FigureFi1g6u.rePr1e6p.aPpreaptiaornatiroonrtoeufet sopfonge-based TOCNFs via crosslinkingofobfPbEPIEanldanTdOCTONFCsNwFitshwCiAthaCsAacarossaslcinrkoers;linker; arrowa(rar)oiws c(aro)sis-linking procpesrso,caesnsd,aanrdroawrro(bw) i(sb)aiusxilari carboxyl addition (this figure isisreprinted with permission from ref. [19fr3o]m.Creofp.y[1r9i3g]h.tC@op2y0r1g7hWt@il2e0y1-7VWChileyV-eVrClahg VGemrlabgHG&mbCHO.&KCGoa.AK,GWaAei,nWheeiinm.h). 8. 1ThhteegprartoegdreInssorogfannaicn/Oocreglalnuilco-sBeabseadseNdasnpocoenlgluelsoissesftoirIDquruitgeDliemliivteerdyin the drug delivery field. NReevceenrtthlye,lmesasg,nseetvicernaalntoycpomespoofsistpesoinngder-ubgasdeedivnearny,opcaerlItuicluolsaerlyhainvecabneceenrtuhseraadpiyn, other biohmadeeddicraalwanpccpolnicssaidtieoranbsl.eFaotternitniostna.nTchee, tXariagoeted adle.lifjV1e9r4yJdfeavnetlitoupmecodsapgoentngset-obwaaserddsCNFs viacammuceltripulsetcisrosusess-licnankibnegcoafrrCieNdFtshrbouyugchelluheloasdevaacnecteodacheytbartied(mCAatAer)iaalnwitahmstiinmouplriooptyl (tri-ethsopxeyci)ficilraenceog(nAitPioTnESch),awrahctiechrstfuicrthtoerpcassvtahreunotlgyhbthonedtaerdgeweidhsistuesrfsaeelec-tmivoedlyi.filNedangoehnyl-amicin thrboruidgshweinthamthienseticmouolrideifneactionens.pTonhdetsoptohnegeexst.ercnoamsptiomsiutleuesx(ex.igb.,itpsHo,utetsmtapnedraitnugrea,nmtial cterial chanthreaeticrcat,epareniusdtticcusaltgtreowanwsotauwrnidtdhs)aSa.snpaduecfruefurictshcaeornmdacellEnet.rrcatohtileoi,inatplolhowywasriiondlsogt9hi 8. ltrnetaetgmreantetsylsnteomrgaanndicth/Oedgruagniscp-eBcaifscieidyNcaannboeciempurloovseedf,ocornDtrriubugtiDngeltioveersyseningsys-temic toxicity. Nonetheless, the drug carrier biocompatibility, immunogenicity, toxicity, resRpeocnesinvtelny,esmsatognmeatgicnnetaicnogrcaodmiepnots,iatensdipnrpdpruergddruelgivrrearnys.ppoarrttaicuilaitrystyililnneceadncmeurcthhere havimepdrroavwemnecon. nsiderable attention. The targeted delivery of antitumor agents towards canceroNuCsCtismsuaeysaclsaon beuctairirzieedatshraonugnophthaertiacdlevcaonacteinghfyobrrcidllmoidaatelrsitaalbwilliityhismtipmrouvlei-or spe-cifimcnerct,obginoideiogracrdhaabrilaiclyte,rbiisotcicosmtpoaptiabsilsittyh,raonudghctehmeitcaarlgefutnecdtisointealsizsaetieocnt.ivReahly.imNiaentoa wit[h19t5h]efusnticmtioulaileizfeedctNrCesCpwonitdh troist(h2e-aemxiteorentahlyls)taimmiunleu(sA(Me.FgC.,)pFHor,Fteem3Op4emraagtunereti,omnaa-gnetic, andnoplattrrtaiscoleusncdoa)tainngd(fAurMthFeCr-NalPtesr).tlhneitiiraplyh,ytshioelnoagnicoaclellhualorsaectuenridsetricwteonrtetloesayslecthhlleortihdeerapeu-tictargeaetnmtewnitthfoar stpries(c2ifi-acmcionnoceethnylr)aatmioinnetofwunacrtdiosntahleizaaffioencte(dAMtisFCuews.aTshcehroesfeonret,othbeetares-atment sysstiegmneadntdotheadmruingosmpeociefiticeistyandancabtieoinmicpchoavreadct,ecroisntitcrsi)j)b.Uthinegrpteosleenscseonfinagmsinyostgermouicp NoinneAthMelFeC5s-N,tPhsewdarsuglinckaerdrietor bthieocmomethpoatrtiebixialitely, (MimTmX,uannoagnetniciaacnitye,rtomximiciuty,n,orseusppornnessisviveeness to madgrnuegt)iccgarrbaodxiyelngtsro,uapnsd. pThroispmerehdthroughwtraasnsmporltoaybeidlityosstuilrlpnaessedthmeuMcThXimlimpriortavtieomnebnyt. kcaeeyNypCionfCGamndtoiacwyannacltshroeborefuf-ugtatdirlegilizveitedsridya.esT-aihnmepadanrcoutpgtoacwrotaicfrildnesecmhoeaantlittnehgyfffcoclearlcsyowrlelhoaicildheeaodlps9tti1am.b2i%izliintwygiittmhhe3p0er.o4ff%vi-ement, bioedffeigcireaendcyaboifidtyr.ubgiolocaodminpgatinbitthietyA,aMnFdCc-hNePms.icTahlefuMnTcXti-oAnMalFizCa-tMioNnP.sRasyhsitmemieetxahli.b[11te9d5] func-tiopnHalirzeesdpoNnsCivCitywiinthwtriisch(2,-aatmaninaoceidhicycl)joanmditnioen(A(pMHFOCF5).f4o),ruFpe3toO749m%aogfntehteicdnruagnowpaasrticles coarteilneagse(Ad,MwFhCile-NovPesr)f.ivIneidtiaaylly,itthexhnbainteodceulplutolo2s9e%undruegrwreelenatsetobsyythcehplororitodneatrtioenatbme-

ent for trish(a2v-
aiomrionfoMetThXylc)jaarmboinxylifcugncrotuiopnsa.lilnzaadtdointio(An,MthFeCnawnaospacrthoicsleesnctoontbtaeinainisngigMneTdXteoxhthibeitami
moaiehtighsearnudptcaakteionficcclcluhlaarracotmerpisatriecds).LoTthheeApMreFsCen-
MceNoPfs,awmhnicohgwreoruepcosnitriAbuMteFdCto-NbyPs was
liinkheedthoemthiecamlseitmhoilrarreixyatoef(MTXw,ainthafnotliiccaanccider(FimAm),wunhoicshupasprisetssitvhee
dirntuegrn)jaclairabtoioxnylogroups. Thrisecmepettohro-
mdewdiaasteedmcpellouyoesde.tTohsiusrepnhasncthesetMheTpXotleimntiitaaloiofnMbTyXkfoerecpainncgerdcoewlntatrhgeetoinfgf-
target sid(eF-igimurpea1c7t)[o1w95a].rds healthy cells while optimizing the efficacy of anticancer drug deliv-
ery. The drug confinement efficacy reached 91.2% with 30.4% efficiency of drug loading in the AMFC-NPs.
The MTX-AMFC-MNPs system exhibited pH responsivity in which, at an acidic condition (pH of 5.4), up to
79% of the drug was released, while over five days, it exhibited up to 29% drug release by the protonation
behavior of MTX carboxylic groups. In addition, the nanoparticles containing MTX exhibit a higher uptake of
cellular Polymers 2021, 13, x compared to the AMFC-MNPs, which were contributed to by the chem40icoafl
4s9imilarity of MTX with folic acid (FA), which assists the internalization of receptor-mediated cellulose. This
enhances the potential of MTX for cancer cell targeting (Figure 17) [195]. (a) (b) Figure17.17(a.)
M(aa)gnMetiagNneCtCic-bNaseCdCn-banaosceadrineranwoitcharprHie-rreswpiothnsivpeHc-
arpeasbpilnhtyisicvoenstraupctaiobnil.itTyheconstruction.
nnTaonhetoehcyenll)lauanmlooisnceeel(wlAuaMlsoFsuCen)dwfeumagscotiinougnnaditoezraygtiloantiin,oginn,ctoworsphyoiclrhaattiinroegna,actmewdir
lcaotmiroidn-e for tris(2- imamprionvoemthenytl,)awmhiinche
(cAonMneFcCte)dfuinntcotitohneamlizetahtoiotrne,xianteco(rMpToXra,tainntgicnaanncienrodmrugi)ectaiersbofxyoyleglerocurposstatic
interac- (MtioTnX@imApMrFoCv@emMNenPts),w;ahnidch(bc)osnchneemctaedic
iinlltuosttrhateiomneothfpoHtr-erxesapteon(sMivTeXa,nadnltoiccaalnizcaetriodnroufgc)jancacerbroxyl groups
tr(eMatTmXe@ntAthMatFbCe@neMfitNedPfsr)jo;manthde(bst)rusccthueramlasitmiciliallruitystrbaettwioenenoffloHhca-
rceidspaonndsMivTeXa,nwdhlicohcaalsisizsattsion of cancer treatment that benefited from the structural
similarity between folic acid and MTX, which assists the folate-receptor-mediated cell internalization (this
figure is redrawn from [195]. Copyright 1987 Royal Society Of Chemistry). Recently, Supramaniam et al.
[196] introduced magnetic characteristics towards nanocellulos-based hydrogels, which were further utilized
for controlling drug deliv- ery. The co-precipitation with Fe (II) and Fe (III) ions was incorporated into the
NCCs, followed by the insertion of the magnetic characteristic, and subsequently, morphologically modified
into beads with sodium alginate. It was observed that the magnetic nanocellu- lose existence refines the
physical and mechanical characteristics of hydrogel beads and swelling degree improvement and limits the
drug release due to the formation of physical entanglement inside the hydrogel. Jeddi and Mahkam [197]
developed magnetic hydro- gel beads composite-based carboxymethyl nanocellulose to deliver
dexamethasone. The composite can control the dexamethasone delivery up to 12 h. Carbon nanotubes
have outstanding characteristics such as high thermal stability, homogenous pore arrangement, high specific
area, and excellent electrical features. This advanced material has also been employed as a vehicle

25in the drug delivery system in recent years. The combination of

this material with the NC material provides some advantages. The incorporation of nanocellulose in the
composite increased biocompatibility and biodegradability while the CNTs provided good stability, magnetic
and electromagnetic behavior, and high cellular uptake [198]. Although the cytotoxicity of material still
became an issue, CNTs were widely exploited in drug delivery systems, particularly cancer therapy
applications [199]. Integration of nanocellulose into graphene-based materials through the layer-by- layer
assembly as a drug carrier was carried out by Anirudhan et al. [200]. Chemically modified GO was used as a
template for the

22layer-by-layer assembly of aminated nano- dextran (AND) and carboxylic acid

functionalized nanocellulose (NCCs) to form a MGO- AND/NCCs nanocomposite. Curcumin can be loaded
into the carrier through π - π stacking and hydrogen bonding interactions due to the phenolic and aromatic
rings of curcumin. Based on the release study, the acidic environment promotes COO- groups' protonation
and amino in aminated in nano-dextran to form NH3+. This phenomenon decreased the static interaction
between MGO-AND/NCC, resulting in the electrostatic repulsion of each component, consequently
provoking the drug release. In addition, a cytotoxicity assay on HCT116 cells exhibited high efficacy of
curcumin-loaded MGO-AND/NCC. The electrochemical activity of the carbon nanotube was utilized

4to modulate the drug release. The release of

ibuprofen from

24a novel hybrid hydrogel composed of sodium alginate (SA), bacterial
cellulose (BC), and multi-walled carbon nanotubes (MWCNTs) was

studied by Shi et al. [176]. The release of ibuprofen can be provoked by electrostatic repul- sion. Thereby,
the on-off release mechanism can be attained by introducing electrochemical potential [176]. 9. Conclusions
Modified and functionalized nanocelluloses with low toxicity and high biocompatibil- ity render them
promising materials as advanced drug carriers. Various hydroxyl groups on the surface of the nanocellulose
serve as attachment sites of drugs through covalent and/or physical interactions. In addition, nanocellulose
modification results in a different morphological structure for the carrier, which contributes to an increase in
the diffusion pathway of the drug within the carrier. Therefore, surface chemistry is a crucial factor that
should be considered in the design

. High-purity nanocelluloses are also required to obtain drug carriers with the well-constructed framework, thus facilitating drug adsorption and release control. Considering all these factors, carrier-based nanocellulose is a promising candidate for developing novel sustained drug delivery systems. Author Contributions: Conceptualization V.B.L., F.E.S. and S.I.; redraw the figures V.B.L. and M.Y.; drafting the manuscript V.B.L., J.N.P., S.P.S. and S.I.; Supervision S.I. and F.E.S.; review and editing, J.S. and Y.H.J.; proof reading J.S. and Y.H.J.

21 All authors have read and agreed to the published version of the manuscript. Funding: This study was supported by the

13 Directorate of Research and Community Service, Deputy for Strengthening Research and Development, Ministry of Research and Technology/National Research and Innovation Agency, Number: 150J/WM01.5/N/2021. Institutional Review Board Statement: Not applicable. Informed Consent Statement: Not applicable

. Conflicts of Interest: The authors declare no conflict of interest. References 1. Jain, K.K. An overview of drug delivery systems. In *Drug Delivery Systems*; Springer: New York, NY, USA, 2020. 2. Sunasee, R.; Hemraz, U.D.; Ckless, K. Cellulose nanocrystals: A versatile nanoplatform for emerging biomedical applications. *Expert Opin. Drug Deliv.* 2016, 13, 1243–1256. [CrossRef] [PubMed] 3. Bamrungsap, S.; Zhao, Z.; Chen, T.; Wand, L.; Li, C.; Fu, T.; Tan, W. Nanotechnology in therapeutics: A focus on nanoparticles as a drug delivery system. *Nanomedicine* 2012, 7, 1253–1271. [CrossRef] 4. Tong, X.; Pan, W.; Su, T.; Zhang, M.; Dong, W.; Qi, X. Recent advances in natural polymer-based drug delivery systems. *React. Funct. Polym.* 2020, 148, 104501. [CrossRef] 5. Cavallaro, G.; Micciulla, S.; Chiappisi, L.; Lazzara, G. Chitosan-based smart hybrid materials: A physico-chemical perspective. *J. Mater. Chem. B* 2021, 9, 594–611. [CrossRef] 6. Bertolino, V.; Cavallaro, G.; Milioto, S.; Lazzara, G. Polysaccharides/Halloysite nanotubes for smart bionanocomposite materials. *Carbohydr. Polym.* 2020, 245, 116502. [CrossRef] 7. Ahmad, A.; Mubarak, N.; Jannat, F.T.; Ashfaq, T.; Santulli, C.; Rizwan, M.; Najda, A.; Bin-Jumah, M.; Abdel-Daim, M.M.; Hussain, S. A Critical Review on the Synthesis of Natural Sodium Alginate Based Composite Materials: An Innovative Biological Polymer for Biomedical Delivery Applications. *Processes* 2021, 9, 137. [CrossRef] 8. Chen, J.; Ouyang, J.; Chen, Q.; Deng, C.; Meng, F.; Zhang, J.; Cheng, R.; Lan, Q.; Zhong, Z. EGFR and CD44 dual-targeted multifunctional hyaluronic acid nanogels boost protein delivery to ovarian and breast cancers in vitro and in vivo. *ACS Appl. Mater. Interfaces* 2017, 9, 24140–24147. [CrossRef] [PubMed] 9. Qi, X.; Wei, W.; Shen, J.; Dong, W. Salecan polysaccharide-based hydrogels and their applications: A review. *J. Mater. Chem. B* 2019, 7, 2577–2587. [CrossRef] [PubMed] 10. Dragan, E.S.; Dinu, M.V. Polysaccharides constructed hydrogels as vehicles for proteins and peptides. A review. *Carbohydr. Polym.* 2019, 225, 115210. [CrossRef] [PubMed] 11. Jorfi, M.; Foster, E.J. Recent advances in nanocellulose for biomedical applications. *J. Appl. Polym. Sci.* 2015, 132, 41719. [CrossRef] 12. Xue, Y.; Mou, Z.; Xiao, H. Nanocellulose as a sustainable biomass material: Structure, properties, present status and future prospects in biomedical applications. *Nanoscale* 2017, 9, 14758–14781. [CrossRef] 13. Habibi, Y.; Lucia, L.A.; Rojas, O.J. Cellulose nanocrystals: Chemistry, self-assembly, and applications. *Chem. Rev.* 2010, 110, 3479–3500. [CrossRef] 14. Lin, N.; Dufresne, A. Nanocellulose in biomedicine: Current status and future prospect. *Eur. Polym. J.* 2014, 59, 302–325. [CrossRef] 15. Plackett, D.; Letchford, K.; Jackson, J.; Burt, H. A review of nanocellulose as a novel vehicle for drug delivery. *Nord. Pulp Pap. Res. J.* 2014, 29, 105–118. [CrossRef] 16. Jawaid, M.; Mohammad, F. *Nanocellulose and Nanohydrogel Matrices: Biotechnological and Biomedical Applications*; John Wiley & Sons: Hoboken, NJ, USA, 2017. 17. Hasan, N.; Rahman, L.; Kim, S.-H.; Cao, J.; Arjuna, A.; Lallo, S.; Jhun, B.H.; Yoo, J.-W. Recent advances of nanocellulose in drug delivery systems. *J. Pharm. Investig.* 2020, 50, 553–572. [CrossRef] 18. Grishkewich, N.; Mohammed, N.; Tang, J.; Tam, K.C. Recent advances in the application of cellulose nanocrystals. *Curr. Opin. Colloid Interface Sci.* 2017, 29, 32–45. [CrossRef] 19. Yan, G.; Chen, B.; Zeng, X.; Sun, Y.; Tan, X.; Lin, L. Recent advances on sustainable cellulosic materials for pharmaceutical carrier applications. *Carbohydr. Polym.* 2020, 244, 116492. [CrossRef] [PubMed] 20. Rajinipriya, M.; Nagalakshmaiah, M.; Robert, M.; Elkoun, S. Importance of agricultural and industrial waste in the field of nanocellulose and recent industrial developments of wood based nanocellulose: A review. *ACS Sustain. Chem. Eng.* 2018, 6, 2807–2828. [CrossRef] 21. Karimian, A.; Parsian, H.; Majidinia, M.; Rahimi, M.; Mir, S.M.; Kafil, H.S.; Shafiei-Irannejad, V.; Kheyrollah, M.; Ostadi, H.; Yousefi, B. Nanocrystalline cellulose: Preparation, physicochemical properties, and applications in drug delivery systems. *Int. J. Biol. Macromol.* 2019, 133, 850–859. [CrossRef] [PubMed] 22. Salimi, S.; Sotudeh-Gharebagh, R.; Zarghami, R.; Chan, S.Y.; Yuen, K.H. Production of nanocellulose and its applications in drug delivery: A critical review. *ACS Sustain. Chem. Eng.* 2019, 7, 15800–15827. [CrossRef] 23. Seabra, A.B.; Bernandes, J.S.; Favaro, W.J.; Paula, A.J.; Duran, N. Cellulose nanocrystals as carriers in medicine and their toxicities: A review. *Carbohydr. Polym.* 2018, 181, 514–527. [CrossRef] [PubMed] 24. Shekhi, A.; Hayashi, J.; Eichenbaum, J.; Gutin, M.; Kuntjoro, N.; Khorsandi, D.; Khademhosseini, A. Recent advances in nanoengineering cellulose for cargo delivery. *J. Control. Release* 2019, 294, 53–76. [CrossRef] [PubMed] 25. Putro, J.N.; Ismadji, S.; Gunarto, C.; Yuliana, M.; Santoso, S.P.; Soetaredjo, F.E.; Ju, Y.H. The effect of surfactants modification on nanocrystalline cellulose for paclitaxel loading and release study. *J. Mol. Liq.* 2019, 282, 407–414. [CrossRef] 26. Bundjaja, V.; Sari, T.M.; Soetaredjo, F.E.; Yuliana, M.; Angkawijaya, A.E.; Ismadji, S.; Cheng, K.-C.; Santoso, S.P. Aqueous sorption of tetracycline using rarasaponin-modified nanocrystalline cellulose. *J. Mol. Liq.* 2020, 301, 112433. [CrossRef] 27. Huang, Y.; Zhu, C.; Yang, J.; Nie, Y.; Chen, C.; Sun, D. Recent advances in bacterial cellulose. *Cellulose* 2014, 21, 1–30. [CrossRef] 28. Foo, M.L.; Tan, C.R.; Lim, P.D.; Ooi, C.W.; Tan, K.W.; Chew, I.M.L. Surface-modified nanocrystalline cellulose

from oil palm empty fruit bunch for effective binding of curcumin. *Int. J. Biol. Macromol.* 2019, 138, 1064–1071. [CrossRef] 29. Wijaya, C.J.; Saputra, S.N.; Soetaredjo, F.E.; Putro, J.N.; Lin, C.X.; Kurniawan, A.; Ju, Y.-H.; Ismadji, S. Cellulose nanocrystals from passion fruit peels waste as antibiotic drug carrier. *Carbohydr. Polym.* 2017, 175, 370–376. [CrossRef] [PubMed] 30. Dufresne, A. Cellulose nanomaterial reinforced polymer nanocomposites. *Curr. Opin. Colloid Interface Sci.* 2017, 29, 1–8. [CrossRef] 31. Gopinath, V.; Saravanan, S.; Al-Maleki, A.; Ramesh, M.; Vadivelu, J. A review of natural polysaccharides for drug delivery applications: Special focus on cellulose, starch and glycogen. *Biomed. Pharmacother.* 2018, 107, 96–108. [CrossRef] 32. Wertz, J.-L.; Bedue, O.; Mercier, J.P. *Cellulose Science and Technology*; EPFL Press: Lausanne, Switzerland, 2010. 33. George, J.; Sabapathi, S. Cellulose nanocrystals: Synthesis, functional properties, and applications. *Nanotechnol. Sci. Appl.* 2015, 8, 45. [CrossRef] 34. Moon, R.J.; Martini, A.; Nairn, J.; Simonsen, J.; Youngblood, J. Cellulose nanomaterials review: Structure, properties and nanocomposites. *Chem. Soc. Rev.* 2011, 40, 3941–3994. [CrossRef] 35. Medronho, B.; Lindman, B. Brief overview on cellulose dissolution/regeneration interactions and mechanisms. *Adv. Colloid Interface Sci.* 2015, 222, 502–508. [CrossRef] 36. Kamel, R.; El-Wakil, N.A.; Dufresne, A.; Elkasabgy, N.A. Nanocellulose: From an agricultural waste to a valuable pharmaceutical ingredient. *Int. J. Biol. Macromol.* 2020, 163, 1579–1590. [CrossRef] [PubMed] 37. Miao, C.; Hamad, W.Y. Cellulose reinforced polymer composites and nanocomposites: A critical review. *Cellulose* 2013, 20, 2221–2262. [CrossRef] 38. Li, N.; Lu, W.; Yu, J.; Xiao, Y.; Liu, S.; Gan, L.; Huang, J. Rod-like cellulose nanocrystal/cis-aconityl-doxorubicin prodrug: A fluorescence-visible drug delivery system with enhanced cellular uptake and intracellular drug controlled release. *Mater. Sci. Eng. C* 2018, 91, 179–189. [CrossRef] [PubMed] 39. Jia, B.; Li, Y.; Yang, B.; Xiao, D.; Zhang, S.; Rajulu, A.V.; Kondo, T.; Zhang, L.; Zhou, J. Effect of microcrystal cellulose and cellulose whisker on biocompatibility of cellulose-based electrospun scaffolds. *Cellulose* 2013, 20, 1911–1923. [CrossRef] 40. Dash, R.; Ragauskas, A.J. Synthesis of a novel cellulose nanowhisker-based drug delivery system. *RSC Adv.* 2012, 2, 3403–3409. [CrossRef] 41. Biswas, S.K.; Sano, H.; Yang, X.; Tanphichai, S.; Shams, M.I.; Yano, H. Highly thermal-resilient AgNW transparent electrode and optical device on thermomechanically superstable cellulose nanorod-reinforced nanocomposites. *Adv. Opt. Mater.* 2019, 7, 1900532. [CrossRef] 42. Wang, N.; Ding, E.; Cheng, R. Thermal degradation behaviors of spherical cellulose nanocrystals with sulfate groups. *Polymer* 2007, 48, 3486–3493. [CrossRef] 43. Ram, B.; Chauhan, G.S.; Mehta, A.; Gupta, R.; Chauhan, K. Spherical nanocellulose-based highly efficient and rapid multifunctional naked-eye Cr(VI) ion chemosensor and adsorbent with mild antimicrobial properties. *Chem. Eng. J.* 2018, 349, 146–155. [CrossRef] 44. Mariano, M.; El Kissi, N.; Dufresne, A. Cellulose nanocrystals and related nanocomposites: Review of some properties and challenges. *J. Polym. Sci. B Polym. Phys.* 2014, 52, 791–806. [CrossRef] 45. Brinchi, L.; Cotana, F.; Fortunati, E.; Kenny, J. Production of nanocrystalline cellulose from lignocellulosic biomass: Technology and applications. *Carbohydr. Polym.* 2013, 94, 154–169. [CrossRef] 46. Phanthong, P.; Reybroycharoen, P.; Hao, X.; Xu, G.; Abudula, A.; Guan, G. Nanocellulose: Extraction and application. *Carbon Resour. Convers.* 2018, 1, 32–43. [CrossRef] 47. Lam, E.; Male, K.B.; Chong, J.H.; Leung, A.C.; Luong, J.H. Applications of functionalized and nanoparticle-modified nanocrystalline cellulose. *Trends Biotechnol.* 2012, 30, 283–290. [CrossRef] [PubMed] 48. Prathapan, R.; Tabor, R.F.; Garnier, G.; Hu, J. Recent progress in cellulose nanocrystal alignment and its applications. *ACS Appl. Bio Mater.* 2020, 3, 1828–1844. [CrossRef] 49. Abitbol, T.; Rivkin, A.; Cao, Y.; Nevo, Y.; Abraham, E.; Ben-Shalom, T.; Lapidot, S.; Shoseyov, O. Nanocellulose, a tiny fiber with huge applications. *Curr. Opin. Biotechnol.* 2016, 39, 76–88. [CrossRef] [PubMed] 50. Henriksson, M.; Henriksson, G.; Berglund, L.; Lindström, T. An environmentally friendly method for enzyme-assisted preparation of microfibrillated cellulose (MFC) nanofibers. *Eur. Polym. J.* 2007, 43, 3434–3441. [CrossRef] 51. Kim, C.-W.; Kim, D.-S.; Kang, S.-Y.; Marquez, M.; Joo, Y.L. Structural studies of electrospun cellulose nanofibers. *Polymer* 2006, 47, 5097–5107. [CrossRef] 52. Dufresne, A. Nanocellulose: A new ageless bionanomaterial. *Mater. Today* 2013, 16, 220–227. [CrossRef] 53. Lavoine, N.; Desloges, I.; Dufresne, A.; Bras, J. Microfibrillated cellulose—Its barrier properties and applications in cellulosic materials: A review. *Carbohydr. Polym.* 2012, 90, 735–764. [CrossRef] 54. Blanco Parte, F.G.; Santoso, S.P.; Chou, C.-C.; Verma, V.; Wang, H.-T.; Ismadji, S.; Cheng, K.-C. Current progress on the production, modification, and applications of bacterial cellulose. *Crit. Rev. Biotechnol.* 2020, 40, 397–414. [CrossRef] [PubMed] 55. Siro, I.; Plackett, D. Microfibrillated cellulose and new nanocomposite materials: A review. *Cellulose* 2010, 17, 459–494. [CrossRef] 56. Huang, J.; Dufresne, A.; Lin, N. *Nanocellulose: From Fundamentals to Advanced Materials*; John Wiley & Sons: Hoboken, NJ, USA, 2019. 57. Jozala, A.F.; De Lencastre-Novaes, L.C.; Lopes, A.M.; De Carvalho Santos-Ebinuma, V.; Mazzola, P.G.; Pessoa-JR, A.; Grotto, D.; Gerenutti, M.; Chaud, M.V. Bacterial nanocellulose production and application: A 10-year overview. *Appl. Microbiol. Biotechnol.* 2016, 100, 2063–2072. [CrossRef] [PubMed] 58. Wei, B.; Yang, G.; Hong, F. Preparation and evaluation of a kind of bacterial cellulose dry films with antibacterial properties. *Carbohydr. Polym.* 2011, 84, 533–538. [CrossRef] 59. Wan, Y.; Wang, J.; Gama, M.; Guo, R.; Zhang, Q.; Zhang, P.; Yao, F.; Luo, H. Biofabrication of a novel bacteria/bacterial cellulose composite for improved adsorption capacity. *Compos. Part A Appl. Sci. Manuf.* 2019, 125, 105560. [CrossRef] 60. Gorgieva, S.; Trcek, J. Bacterial cellulose: Production, modification and perspectives in biomedical applications. *Nanomaterials* 2019, 9, 1352. [CrossRef] [PubMed] 61. Kim, J.-H.; Shim, B.S.; Kim, H.S.; Lee, Y.-J.; Min, S.-K.; Jang, D.; Abas, Z.; Kim, J. Review of nanocellulose for sustainable future materials. *Int. J. Precis. Eng. Manuf. Green Technol.* 2015, 2, 197–213. [CrossRef] 62. Dufresne, A. Cellulose-based composites and nanocomposites. In *Monomers, Polymers, and Composites from Renewable Resources*; Elsevier: Amsterdam, The Netherlands, 2008. 63. Song, F.; Li, X.; Wang, Q.; Liao, L.; Zhang, C. Nanocomposite hydrogels and their applications in drug delivery and tissue engineering. *J. Biomed. Nanotechnol.* 2015, 11, 40–52. [CrossRef] 64. Ibrahim, M.M.; Fahmy, T.Y.; Salaheldin, E.I.; Mobarak, F.; Youssef, M.A.; Mabrook, M.R. Synthesis of tosylated and trimethylsilylated methyl cellulose as pH-sensitive carrier matrix. *Life Sci. J.* 2015, 1, 29–37. 65. Ximenes, F.A.; Gardner, W.D.; Katuria, A. Proportion of above-ground biomass in commercial logs and residues following the harvest of five commercial forest species in Australia. *For. Ecol. Manag.* 2008, 256, 335–346. [CrossRef] 66. Kargarzadeh, H.; Iloelovich, M.; Ahmad, I.; Thomas, S.; Dufresne, A. Methods for extraction of nanocellulose from various sources. *Handb. Nanocellulose Cellul. Nanocomposites* 2017, 2, 1–49. 67. Kumar, A.K.; Sharma, S. Recent updates on different methods of pretreatment of lignocellulosic feedstocks: A review. *Bioresour. Bioproc.* 2017, 4, 1–19. [CrossRef] 68. Ravindran, R.; Jaiswal, S.; Abu-Ghannam, N.; Jaiswal, A.K. A comparative analysis of pretreatment strategies on the properties and hydrolysis of brewers' spent grain. *Bioresour. Technol.* 2018,

248, 272–279. [CrossRef] [PubMed] 69. Pires, J.R.; De Souza, V.G.L.; Fernando, A.L. Production of nanocellulose from lignocellulosic biomass wastes: Prospects and limitations. In Proceedings of the International Conference on Innovation, Engineering and Entrepreneurship, Guimaraes, Portugal, 27–29 June 2018; pp. 719–725. 70. Shirkavand, E.; Baroutian, S.; Gapes, D.J.; Young, B.R. Combination of fungal and physicochemical processes for lignocellulosic biomass pretreatment—A review. *Renew. Sust. Energy Rev.* 2016, 54, 217–234. [CrossRef] 71. Baramée, S.; Siriatcharanon, A.-K.; Ketbot, P.; Teeravivattanakit, T.; Waeonukul, R.; Pason, P.; Tachaapaikoon, C.; Ratanakhanokchai, K.; Phitsuwan, P. Biological pretreatment of rice straw with cellulase-free xylanolytic enzyme-producing *Bacillus firmus* K-1: Structural modification and biomass digestibility. *Renew. Energy* 2020, 160, 555–563. [CrossRef] 72. Khaili, H.A.; Davoudpour, Y.; Islam, M.N.; Mustapha, A.; Sudesh, K.; Dungani, R.; Jawaid, M. Production and modification of nanofibrillated cellulose using various mechanical processes: A review. *Carbohydr. Polym.* 2014, 99, 649–665. [CrossRef] 73. Mood, S.H.; Golfeshan, A.H.; Tabatabaei, M.; Jouzani, G.S.; Najafi, G.H.; Gholami, M.; Ardjmand, M. Lignocellulosic biomass to bioethanol, a comprehensive review with a focus on pretreatment. *Renew. Sust. Energy Rev.* 2013, 27, 77–93. [CrossRef] 74. Hassan, S.S.; Williams, G.A.; Jaiswal, A.K. Emerging technologies for the pretreatment of lignocellulosic biomass. *Bioresour. Technol.* 2018, 262, 310–318. [CrossRef] 75. De Carvalho Benini, K.C.C.; Voorwald, H.J.C.; Cioffi, M.O.H.; Rezende, M.C.; Arantes, V. Preparation of nanocellulose from *Imperata brasiliensis* grass using Taguchi method. *Carbohydr. Polym.* 2018, 192, 337–346. [CrossRef] 76. Maciel, M.M.Á.D.; De Carvalho Benini, K.C.C.; Voorwald, H.J.C.; Cioffi, M.O.H. Obtainment and characterization of nanocellulose from an unwoven industrial textile cotton waste: Effect of acid hydrolysis conditions. *Int. J. Biol. Macromol.* 2019, 126, 496–506. [CrossRef] 77. Liu, J.; Korpinen, R.; Mikkonen, K.S.; Willför, S.; Xu, C. Nanofibrillated cellulose originated from birch sawdust after sequential extractions: A promising polymeric material from waste to films. *Cellulose* 2014, 21, 2587–2598. [CrossRef] 78. Couret, L.; Irie, M.; Belloncle, C.; Cathala, B. Extraction and characterization of cellulose nanocrystals from post-consumer wood fiberboard waste. *Cellulose* 2017, 24, 2125–2137. [CrossRef] 79. Vallejos, M.E.; Felissia, F.E.; Area, M.C.; Ehman, N.V.; Tarrés, Q.; Mutjé, P. Nanofibrillated cellulose (CNF) from eucalyptus sawdust as a dry strength agent of unrefined eucalyptus handsheets. *Carbohydr. Polym.* 2016, 139, 99–105. [CrossRef] [PubMed] 80. Rambabu, N.; Panthapulakkal, S.; Sain, M.; Dalai, A. 2016. Production of nanocellulose fibers from pinecone biomass: Evaluation and optimization of chemical and mechanical treatment conditions on mechanical properties of nanocellulose films. *Ind. Crops Prod.* 2016, 83, 746–754. [CrossRef] 81. Moriana, R.; Vilaplana, F.; Ek, M. Cellulose nanocrystals from forest residues as reinforcing agents for composites: A study from macro-to nano-dimensions. *Carbohydr. Polym.* 2016, 139, 139–149. [CrossRef] 82. Lu, H.; Zhang, L.; Liu, C.; He, Z.; Zhou, X.; Ni, Y. A novel method to prepare lignocellulose nanofibrils directly from bamboo chips. *Cellulose* 2018, 25, 7043–7051. [CrossRef] 83. Hua, K.; Strømme, M.; Mihranyan, A.; Ferraz, N. Nanocellulose from green algae modulates the in vitro inflammatory response of monocytes/macrophages. *Cellulose* 2015, 22, 3673–3688. [CrossRef] 84. Son, H.N.; Seo, Y.B. Physical and bio-composite properties of nanocrystalline cellulose from wood, cotton liners, cattail, and red algae. *Cellulose* 2015, 22, 1789–1798. 85. Rathod, M.; Haldar, S.; Basha, S. Nanocrystalline cellulose for removal of tetracycline hydrochloride from water via biosorption: Equilibrium, kinetic and thermodynamic studies. *Ecol. Eng.* 2015, 84, 240–249. [CrossRef] 86. Liu, Z.; Li, X.; Xie, W.; Deng, H. Extraction, isolation and characterization of nanocrystalline cellulose from industrial kelp (*Laminaria japonica*) waste. *Carbohydr. Polym.* 2017, 173, 353–359. [CrossRef] [PubMed] 87. Feng, X.; Meng, X.; Zhao, J.; Miao, M.; Shi, L.; Zhang, S.; Fang, J. Extraction and preparation of cellulose nanocrystals from dealginate kelp residue: Structures and morphological characterization. *Cellulose* 2015, 22, 1763–1772. [CrossRef] 88. Bhutiya, P.L.; Misra, N.; Rasheed, M.A.; Hasan, S.Z. Nested seaweed cellulose fiber deposited with cuprous oxide nanorods for antimicrobial activity. *Int. J. Biol. Macromol.* 2018, 117, 435–444. [CrossRef] 89. De Oliveira, J.P.; Bruni, G.P.; Fabra, M.J.; Da Rosa Zavareze, E.; López-Rubio, A.; Martínez-Sanz, M. Development of food packaging bioactive aerogels through the valorization of *Gelidium sesquipedale* seaweed. *Food Hydrocoll.* 2019, 89, 337–350. [CrossRef] 90. Chen, Y.W.; Lee, H.V.; Juan, J.C.; Phang, S.-M. Production of new cellulose nanomaterial from red algae marine biomass *Gelidium elegans*. *Carbohydr. Polym.* 2016, 151, 1210–1219. [CrossRef] [PubMed] 91. Mandal, A.; Chakrabarty, D. Isolation of nanocellulose from waste sugarcane bagasse (SCB) and its characterization. *Carbohydr. Polym.* 2011, 86, 1291–1299. [CrossRef] 92. Thomas, M.G.; Abraham, E.; Jyotishkumar, P.; Maria, H.J.; Pothan, L.A.; Thomas, S. Nanocelluloses from jute fibers and their nanocomposites with natural rubber: Preparation and characterization. *Int. J. Biol. Macromol.* 2015, 81, 768–777. [CrossRef] [PubMed] 93. Wu, J.; Du, X.; Yin, Z.; Xu, S.; Xu, S.; Zhang, Y. Preparation and characterization of cellulose nanofibrils from coconut coir fibers and their reinforcements in biodegradable composite films. *Carbohydr. Polym.* 2019, 211, 49–56. [CrossRef] [PubMed] 94. Mariño, M.; Lopes Da Silva, L.; Durán, N.; Tasic, L. Enhanced materials from nature: Nanocellulose from citrus waste. *Molecules* 2015, 20, 5908–5923. [CrossRef] 95. Dilamian, M.; Noroozi, B. A combined homogenization-high intensity ultrasonication process for individualizaion of cellulose micro-nano fibers from rice straw. *Cellulose* 2019, 26, 5831–5849. [CrossRef] 96. Kang, X.; Sun, P.; Kuga, S.; Wang, C.; Zhao, Y.; Wu, M.; Huang, Y. Thin cellulose nanofiber from corncob cellulose and its performance in transparent nanopaper. *ACS Sust. Chem. Eng.* 2017, 5, 2529–2534. [CrossRef] 97. Karimi, S.; Tahir, P.M.; Karimi, A.; Dufresne, A.; Abdulkhani, A. Kenaf bast cellulosic fibers hierarchy: A comprehensive approach from micro to nano. *Carbohydr. Polym.* 2014, 101, 878–885. [CrossRef] 98. Jodeh, S.; Hamed, O.; Melhem, A.; Salghi, R.; Jodeh, D.; Azzaoui, K.; Benmassaoud, Y.; Murtada, K. Magnetic nanocellulose from olive industry solid waste for the effective removal of methylene blue from wastewater. *Environ. Sci. Poll. Res.* 2018, 25, 22060–22074. [CrossRef] 99. Jongaroontaprangsee, S.; Chiewchan, N.; Devahastin, S. Production of nanofibrillated cellulose with superior water redispersibility from lime residues via a chemical-free process. *Carbohydr. Polym.* 2018, 193, 249–258. [CrossRef] [PubMed] 100. Diop, C.I.K.; Lavoie, J.-M. Isolation of nanocrystalline cellulose: A technological route for valorizing recycled tetra pak aseptic multilayered food packaging wastes. *Waste Biomass Valor.* 2017, 8, 41–56. [CrossRef] 101. Putro, J.N.; Santoso, S.P.; Soetaredjo, F.E.; Ismadji, S.; Ju, Y.-H. Nanocrystalline cellulose from waste paper: Adsorbent for azo dyes removal. *Environ. Nanotech. Monit. Manag.* 2019, 12, 100260. [CrossRef] 102. Ogundare, S.A.; Moodley, V.; Van Zyl, W.E. Nanocrystalline cellulose isolated from discarded cigarette filters. *Carbohydr. Polym.* 2017, 175, 273–281. [CrossRef] [PubMed] 103. Peretz, R.; Sterenzon, E.; Gerchman, Y.; Vadivel, V.K.; Luxbacher, T.; Mamane, H. Nanocellulose production from recycled paper mill sludge using ozonation pretreatment followed by recyclable maleic acid hydrolysis. *Carbohydr. Polym.* 2019, 216, 343–351.

[CrossRef] [PubMed] 104. Cypriano, D.Z.; Da Silva, L.L.; Tasic, L. High value-added products from the orange juice industry waste. *Waste Manag.* 2018, 79, 71–78. [CrossRef] [PubMed] 105. Dubey, S.; Singh, J.; Singh, R. Biotransformation of sweet lime pulp waste into high-quality nanocellulose with an excellent productivity using *Komagataeibacter europaeus* SGP37 under static intermittent fed-batch cultivation. *Bioresour. Technol.* 2018, 247, 73–80. [CrossRef] [PubMed] 106. Mondal, S. Preparation, properties and applications of nanocellulosic materials. *Carbohydr. Polym.* 2017, 163, 301–316. [CrossRef] 107. Turbak, A.F.; Snyder, F.W.; Sandberg, K.R. Microfibrillated cellulose, a new cellulose product: Properties, uses, and commercial potential. *J. Appl. Polym. Sci. Appl. Polym. Sym.* 1983, 37, 815–827. 108. Herrick, F.W.; Casebier, R.L.; Hamilton, J.K.; Sandberg, K.R. Microfibrillated cellulose: Morphology and accessibility. *J. Appl. Polym. Sci. Appl. Polym. Sym.* 1983, 37, 797–813. 109. Kawee, N.; Lam, N.T.; Sukyai, P. Homogenous isolation of individualized bacterial nanofibrillated cellulose by high pressure homogenization. *Carbohydr. Polym.* 2018, 179, 394–401. [CrossRef] 110. Yusra, A.I.; Juahir, H.; Firdaus, N.N.A.; Bhat, A.; Endut, A.; Khalil, H.A.; Adiana, G. Controlling of green nanocellulose fiber properties produced by chemo-mechanical treatment process via SEM, TEM, AFM and image analyzer characterization. *J. Fund. Appl. Sci.* 2018, 10, 1–17. 111. Kalia, S.; Boufi, S.; Celli, A.; Kango, S. Nanofibrillated cellulose: Surface modification and potential applications. *Colloid Polym. Sci.* 2014, 292, 5–31. [CrossRef] 112. Niu, F.; Li, M.; Huang, Q.; Zhang, X.; Pan, W.; Yang, J.; Li, J. The characteristic and dispersion stability of nanocellulose produced by mixed acid hydrolysis and ultrasonic assistance. *Carbohydr. Polym.* 2017, 165, 197–204. [CrossRef] [PubMed] 113. Trache, D.; Hussin, M.H.; Haafiz, M.M.; Thakur, V.K. Recent progress in cellulose nanocrystals: Sources and production. *Nanoscale* 2017, 9, 1763–1786. [CrossRef] 114. Wang, J.; Tavakoli, J.; Tang, Y. Bacterial cellulose production, properties and applications with different culture methods—A review. *Carbohydr. Polym.* 2019, 219, 63–76. [CrossRef] 115. Czaja, W.; Romanovicz, D.; Malcolm, B.R. Structural investigations of microbial cellulose produced in stationary and agitated culture. *Cellulose* 2004, 11, 403–411. [CrossRef] 116. Matsutani, M.; Ito, K.; Azuma, Y.; Ogino, H.; Shirai, M.; Yakushi, T.; Matsushita, K. Adaptive mutation related to cellulose producibility in *Komagataeibacter medellinensis* (*Gluconacetobacter xylinus*) NBRC 3288. *Appl. Microbiol. Biotechnol.* 2015, 99, 7229–7240. [CrossRef] [PubMed] 117. Liu, M.; Zhong, C.; Wu, X.-Y.; Wei, Y.-Q.; Bo, T.; Han, P.-P.; Jia, S.-R. Metabolomic profiling coupled with metabolic network reveals differences in *Gluconacetobacter xylinus* from static and agitated cultures. *Biochem. Eng. J.* 2015, 101, 85–98. [CrossRef] 118. Gullo, M.; La China, S.; Petroni, G.; Di Gregorio, S.; Giudici, P. Exploring K2G30 genome: A high bacterial cellulose producing strain in glucose and mannitol based media. *Front. Microbiol.* 2019, 10, 58. [CrossRef] [PubMed] 119. Thorat, M.N.; Dastager, S.G. High yield production of cellulose by a *Komagataeibacter rhaeticus* PG2 strain isolated from pomegranate as a new host. *RSC Adv.* 2018, 8, 29797–29805. [CrossRef] 120. Volova, T.G.; Prudnikova, S.V.; Sukovaty, A.G.; Shishatskaya, E.I. Production and properties of bacterial cellulose by the strain *Komagataeibacter xylinus* B-12068. *Appl. Microbiol. Biotechnol.* 2018, 102, 7417–7428. [CrossRef] [PubMed] 121. Molina-Ramírez, C.; Castro, M.; Osorio, M.; Torres-Taborda, M.; Gómez, B.; Zuluaga, R.; Gómez, C.; Gañán, P.; Rojas, O.J.; Castro, C. Effect of different carbon sources on bacterial nanocellulose production and structure using the low pH resistant strain *Komagataeibacter medellinensis*. *Materials* 2017, 10, 639. [CrossRef] 122. Mohammadkazemi, F.; Azin, M.; Ashori, A. Production of bacterial cellulose using different carbon sources and culture media. *Carbohydr. Polym.* 2015, 117, 518–523. [CrossRef] [PubMed] 123. Mitchell, M.J.; Billingsley, M.M.; Haley, R.M.; Wechsler, M.E.; Peppas, N.A.; Langer, R. Engineering precision nanoparticles for drug delivery. *Nat. Rev. Drug Discov.* 2020, 20, 101–124. [CrossRef] [PubMed] 124. Hare, J.I.; Lammers, T.; Ashford, M.B.; Puri, S.; Strom, G.; Barry, S.T. Challenges and strategies in anti-cancer nanomedicine development: An industry perspective. *Adv. Drug Deliv. Rev.* 2017, 108, 25–38. [CrossRef] [PubMed] 125. Araki, J. Electrostatic or steric?—preparations and characterizations of well-dispersed systems containing rod-like nanowhiskers of crystalline polysaccharides. *Soft Mater.* 2013, 9, 4125–4141. [CrossRef] 126. Kargarzadeh, H.; Mariano, M.; Gopakumar, D.; Ahmad, I.; Thomas, S.; Dufresne, A.; Huang, J.; Lin, N. Advances in cellulose nanomaterials. *Cellulose* 2018, 25, 2151–2189. [CrossRef] 127. Hebeish, A.; Guthrie, T. *The Chemistry and Technology of Cellulosic Copolymers*; Springer Science & Business Media: Berlin, Germany, 2012. 128. De La Motte, H.; Hasani, M.; Brelid, H.; Westman, G. Molecular characterization of hydrolyzed cationized nanocrystalline cellulose, cotton cellulose and softwood kraft pulp using high resolution 1D and 2D NMR. *Carbohydr. Polym.* 2011, 85, 738–746. [CrossRef] 129. Habibi, Y. Key advances in the chemical modification of nanocelluloses. *Chem. Soc. Rev.* 2014, 43, 1519–1542. [CrossRef] 130. Pakhareenko, V.; Pervaiz, M.; Pande, H.; Sain, M.; Sain, M. Chemical and physical techniques for surface modification of nanocellulose reinforcements. In *Interface/Interphase in Polymer Nanocomposites*; John Wiley & Sons: Hoboken, NJ, USA, 2016; pp. 283–310. 131. Meneguín, A.B.; da Silva Barud, H.; Sabio, R.M.; de Sousa, P.Z.; Manieri, K.F.; de Freitas, L.A.P.; Pacheco, G.; Alonso, J.D.; Chorilli, M. Spray-dried bacterial cellulose nanofibers: A new generation of pharmaceutical excipient intended for intestinal drug delivery. *Carbohydr. Polym.* 2020, 249, 116838. [CrossRef] 132. Khine, Y.Y.; Stenzel, M.H. Surface modified cellulose nanomaterials: A source of non-spherical nanoparticles for drug delivery. *Mater. Horiz.* 2020, 7, 1727–1758. [CrossRef] 133. Kusano, Y.; Madsen, B.; Berglund, L.; Oksman, K. Modification of cellulose nanofibre surfaces by He/NH₃ plasma at atmospheric pressure. *Cellulose* 2019, 26, 7185–7194. [CrossRef] 134. Taheri, A.; Mohammadi, M. The use of cellulose nanocrystals for potential application in topical delivery of hydroquinone. *Chem. Biol. Drug Design* 2015, 86, 102–106. [CrossRef] [PubMed] 135. Camarero Espinosa, S.; Kuhnt, T.; Foster, E.J.; Weder, C. Isolation of thermally stable cellulose nanocrystals by phosphoric acid hydrolysis. *Biomacromol.* 2013, 14, 1223–1230. [CrossRef] 136. Wang, N.; Ding, E.; Cheng, R. Preparation and liquid crystalline properties of spherical cellulose nanocrystals. *Langmuir* 2008, 24, 5–8. [CrossRef] [PubMed] 137. Lin, N.; Dufresne, A. Surface chemistry, morphological analysis and properties of cellulose nanocrystals with gradiented sulfation degrees. *Nanoscale* 2014, 6, 5384–5393. [CrossRef] 138. Kokol, V.; Božič, M.; Vogrinčić, R.; Mathew, A.P. Characterisation and properties of homo- and heterogeneously phosphorylated nanocellulose. *Carbohydr. Polym.* 2015, 125, 301–313. [CrossRef] 139. Wang, H.; Xie, H.; Du, H.; Wang, X.; Liu, W.; Duan, Y.; Zhang, X.; Sun, L.; Zhang, X.; Si, C. Highly efficient preparation of functional and thermostable cellulose nanocrystals via H₂SO₄ intensified acetic acid hydrolysis. *Carbohydr. Polym.* 2020, 239, 116233. [CrossRef] 140. Braun, B.; Dorgan, J.R. Single-step method for the isolation and surface functionalization of cellulosic nanowhiskers. *Biomacromolecules* 2009, 10, 334–341. [CrossRef] [PubMed] 141. Chen, G.-Y.; Yu, H.-Y.; Zhang, C.-H.; Zhou, Y.; Yao, J.-M. A universal route for the simultaneous extraction and functionalization of

cellulose nanocrystals from industrial and agricultural celluloses. *J. Nanopart. Res.* 2016, 18, 48. [CrossRef] 142. Du, H.; Liu, C.; Mu, X.; Gong, W.; Lv, D.; Hong, Y.; Si, C.; Li, B. Preparation and characterization of thermally stable cellulose nanocrystals via a sustainable approach of FeCl₃-catalyzed formic acid hydrolysis. *Cellulose* 2016, 23, 2389–2407. [CrossRef] 143. Spinella, S.; Re, G.L.; Liu, B.; Dorgan, J.; Habibi, Y.; Leclere, P.; Raquez, J.-M.; Dubois, P.; Gross, R.A. Poly(lactide)/cellulose nanocrystal nanocomposites: Efficient routes for nanofiber modification and effects of nanofiber chemistry on PLA reinforcement. *Polymer* 2015, 65, 9–17. [CrossRef] 144. Chen, L.; Zhu, J.Y.; Baez, C.; Kitin, P.; Elder, T. Highly thermal-stable and functional cellulose nanocrystals and nanofibrils produced using fully recyclable organic acids. *Green Chem.* 2016, 18, 3835–3843. [CrossRef] 145. Bian, H.; Chen, L.; Dai, H.; Zhu, J. Integrated production of lignin containing cellulose nanocrystals (LCNC) and nanofibrils (LCNF) using an easily recyclable di-carboxylic acid. *Carbohydr. Polym.* 2017, 167, 167–176. [CrossRef] 146. Jia, W.; Liu, Y. Two characteristic cellulose nanocrystals (CNCs) obtained from oxalic acid and sulfuric acid processing. *Cellulose* 2019, 26, 8351–8365. [CrossRef] 147. Luo, J.; Huang, K.; Xu, Y.; Fan, Y. A comparative study of lignocellulosic nanofibrils isolated from celery using oxalic acid hydrolysis followed by sonication and mechanical fibrillation. *Cellulose* 2019, 26, 5237–5246. [CrossRef] 148. Spinella, S.; Maiorana, A.; Qian, Q.; Dawson, N.J.; Hepworth, V.; Mccallum, S.A.; Ganesh, M.; Singer, K.D.; Gross, R.A. 2016. Concurrent cellulose hydrolysis and esterification to prepare a surface-modified cellulose nanocrystal decorated with carboxylic acid moieties. *ACS Sust. Chem. Eng.* 2016, 4, 1538–1550. [CrossRef] 149. Ji, H.; Xiang, Z.; Qi, H.; Han, T.; Pranovich, A.; Song, T. Strategy towards one-step preparation of carboxylic cellulose nanocrystals and nanofibrils with high yield, carboxylation and highly stable dispersibility using innocuous citric acid. *Green Chem.* 2019, 21, 1956–1964. [CrossRef] 150. Habibi, Y.; Chanzy, H.; Vignon, M.R. TEMPO-mediated surface oxidation of cellulose whiskers. *Cellulose* 2006, 13, 679–687. [CrossRef] 151. Jiang, J.; Ye, W.; Liu, L.; Wang, Z.; Fan, Y.; Saito, T.; Isogai, A. Cellulose nanofibers prepared using the TEMPO/laccase/O₂ system. *Biomacromolecules* 2017, 18, 288–294. [CrossRef] [PubMed] 152. Plappert, S.F.; Liebner, F.W.; Konnerth, J.; Nedelec, J.-M. Anisotropic nanocellulose gel-membranes for drug delivery: Tailoring structure and interface by sequential periodate–chlorite oxidation. *Carbohydr. Polym.* 2019, 226, 115306. [CrossRef] [PubMed] 153. Mascheroni, E.; Rampazzo, R.; Ortenzi, M.A.; Piva, G.; Bonetti, S.; Piergiovanni, L. Comparison of cellulose nanocrystals obtained by sulfuric acid hydrolysis and ammonium persulfate, to be used as coating on flexible food-packaging materials. *Cellulose* 2016, 23, 779–793. [CrossRef] 154. Montanari, S.; Roumani, M.; Heux, L.; Vignon, M.R. Topochemistry of carboxylated cellulose nanocrystals resulting from TEMPO-mediated oxidation. *Macromolecules* 2005, 38, 1665–1671. [CrossRef] 155. Carlsson, D.O.; Hua, K.; Forsgren, J.; Mihranyan, A. Aspirin degradation in surface-charged TEMPO-oxidized mesoporous crystalline nanocellulose. *Int. J. Pharm.* 2014, 461, 74–81. [CrossRef] 156. Chen, X.; Xu, X.; Li, W.; Sun, B.; Yan, J.; Chen, C.; Liu, J.; Qian, J.; Sun, D. Effective drug carrier based on poly(ethyleneimine)-functionalized bacterial cellulose with controllable release properties. *ACS Appl. Bio Mater.* 2018, 1, 42–50. [CrossRef] 157. Singhsa, P.; Narain, R.; Manuspiya, H. Bacterial cellulose nanocrystals (BNCC) preparation and characterization from three bacterial cellulose sources and development of functionalized BNCCs as nucleic acid delivery systems. *ACS Appl. Nano Mater.* 2017, 1, 209–221. [CrossRef] 158. Li, L.; Yu, C.; Yu, C.; Chen, Q.; Yu, S. Nanocellulose as template to prepare rough-hydroxy rich hollow silicon mesoporous nanospheres (R-nCHMSNs) for drug delivery. *Int. J. Biol. Macromol.* 2021, 180, 432–438. [CrossRef] 159. Akhlaghi, S.P.; Berry, R.C.; Tam, K.C. Surface modification of cellulose nanocrystal with chitosan oligosaccharide for drug delivery applications. *Cellulose* 2013, 20, 1747–1764. [CrossRef] 160. Tortorella, S.; Maturi, M.; Dapporto, F.; Spanu, C.; Sambri, L.; Franchini, M.C.; Chiariello, M.; Locatelli, E. Surface modification of nanocellulose through carbamate link for a selective release of chemotherapeutics. *Cellulose* 2020, 27, 8503–8511. [CrossRef] 161. Liu, Y.; Sui, Y.; Liu, C.; Liu, C.; Wu, M.; Li, B.; Li, Y. A physically crosslinked polydopamine/nanocellulose hydrogel as potential versatile vehicles for drug delivery and wound healing. *Carbohydr. Polym.* 2018, 188, 27–36. [CrossRef] [PubMed] 162. Wang, H.; He, J.; Zhang, M.; Tam, K.C.; Ni, P. A new pathway towards polymer modified cellulose nanocrystals via a “grafting onto” process for drug delivery. *Polym. Chem.* 2015, 6, 4206–4209. [CrossRef] 163. Kumar, A.; Durand, H.; Zeno, E.; Balsollier, C.; Watbled, B.; Sillard, C.; Fort, S.; Baussanne, I.; Belgacem, N.; Lee, D. The surface chemistry of a nanocellulose drug carrier unraveled by MAS-DNP. *Chem. Sci.* 2020, 11, 3868–3877. [CrossRef] [PubMed] 164. Khine, Y.Y.; Ganda, S.; Stenzel, M.H. Covalent tethering of temperature responsive pNIPAm onto TEMPO-oxidized cellulose nanofibrils via three-component passerini reaction. *ACS Macro Lett.* 2018, 7, 412–418. [CrossRef] 165. Tardy, B.L.; Yokota, S.; Ago, M.; Xiang, W.; Kondo, T.; Bordes, R.; Rojas, O.J. Nanocellulose–surfactant interactions. *Curr. Opin. Colloid Interface Sci.* 2017, 29, 57–67. [CrossRef] 166. Zainuddin, N.; Ahmad, I.; Kargazadeh, H.; Ramli, S. Hydrophobic kenaf nanocrystalline cellulose for the binding of curcumin. *Carbohydr. Polym.* 2017, 163, 261–269. [CrossRef] 167. Raghav, N.; Sharma, M.R. Usage of nanocrystalline cellulose phosphate as novel sustained release system for anti-inflammatory drugs. *J. Mol. Struct.* 2021, 1233, 130108. [CrossRef] 168. Gupta, R.D.; Raghav, N. Differential effect of surfactants tetra-n-butyl ammonium bromide and N-Cetyl-N,N,N-trimethyl ammonium bromide bound to nano-cellulose on binding and sustained release of some non-steroidal anti-inflammatory drugs. *Int. J. Biol. Macromol.* 2020, 164, 2745–2752. [CrossRef] 169. Liu, X.Q.; Picart, C. Layer-by-layer assemblies for cancer treatment and diagnosis. *Adv. Mater.* 2016, 28, 1295–1301. [CrossRef] [PubMed] 170. De Koker, S.; Hoogenboom, R.; De Geest, B.G. Polymeric multilayer capsules for drug delivery. *Chem. Soc. Rev.* 2012, 41, 2867–2884. [CrossRef] 171. Eivazi, A.; Medronho, B.; Lindman, B.; Norgren, M. On the development of all-cellulose capsules by vesicle-templated layer-by-layer assembly. *Polymers* 2021, 13, 589. [CrossRef] 172. Kulkarni, A.D.; Vanjari, Y.H.; Sanchei, K.H.; Patel, H.M.; Belgamwar, V.S.; Surana, S.J.; Pardeshi, C.V. Polyelectrolyte complexes: Mechanisms, critical experimental aspects, and applications. *Artif. Cells Nanomed. Biotechnol.* 2016, 44, 1615–1625. [CrossRef] 173. Mohanta, V.; Madras, G.; Patil, S. Layer-by-layer assembled thin films and microcapsules of nanocrystalline cellulose for hydrophobic drug delivery. *ACS Appl. Mater. Interfaces* 2014, 6, 20093–20101. [CrossRef] [PubMed] 174. Li, J.; Wang, Y.; Zhang, L.; Xu, Z.; Dai, H.; Wu, W. Nanocellulose/gelatin composite cryogels for controlled drug release. *ACS Sust. Chem. Eng.* 2019, 7, 6381–6389. [CrossRef] 175. Hennink, W.E.; Van Nostrum, C.F. Novel crosslinking methods to design hydrogels. *Adv. Drug Deliv. Rev.* 2012, 64, 223–236. [CrossRef] 176. Shi, X.; Zheng, Y.; Wang, G.; Lin, Q.; Fan, J. pH-and electro-response characteristics of dual control cellulose nanofiber/sodium alginate hybrid hydrogels for buccal controlled drug delivery. *RSC Adv.* 2014, 4, 47056–47065. [CrossRef] 177. Lin, N.; Geze, A.; Wouessidjewe, D.; Huang, J.; Dufresne, A.

Biocompatible double-membrane hydrogels from cationic cellulose nanocrystals and anionic alginate as complexing drugs codelivery. *ACS Appl. Mater. Interfaces* 2016, 8, 6880–6889. [CrossRef] 178. Lin, N.; Dufresne, A. Supramolecular hydrogels from in situ host–guest inclusion between chemically modified cellulose nanocrystals and cyclodextrin. *Biomacromolecules* 2013, 14, 871–880. [CrossRef] 179. Muller, A.; Ni, Z.; Hessler, N.; Wesarg, F.; Muller, F.A.; Kralisch, D.; Fischer, D. The biopolymer bacterial nanocellulose as drug delivery system: Investigation of drug loading and release using the model protein albumin. *J. Pharma. Sci.* 2013, 102, 579–592. [CrossRef] 180. Muller, A.; Zink, M.; Hessler, N.; Wesarg, F.; Muller, F.A.; Kralisch, D.; Fischer, D. Bacterial nanocellulose with a shape-memory effect as potential drug delivery system. *RSC Adv.* 2014, 4, 57173–57184. [CrossRef] 181. Kopac, T.; Krajnc, M.; Ručigaj, A. A mathematical model for pH-responsive ionically crosslinked TEMPO nanocellulose hydrogel design in drug delivery systems. *Int. J. Biol. Macromol.* 2021, 168, 695–707. [CrossRef] [PubMed] 182. Jiang, S.; Agarwal, S.; Greiner, A. Low-density open cellular sponges as functional materials. *Angew. Chem. Int. Ed.* 2017, 56, 15520–15538. [CrossRef] [PubMed] 183. Lavoine, N.; Bergstrom, L. Nanocellulose-based foams and aerogels: Processing, properties, and applications. *J. Mater. Chem. A* 2017, 5, 16105–16117. [CrossRef] 184. Pierre, A.C.; Pajonk, G.M. Chemistry of aerogels and their applications. *Chem. Rev.* 2002, 102, 4243–4266. [CrossRef] 185. Kargarzadeh, H.; Huang, J.; Lin, N.; Ahmad, I.; Mariano, M.; Dufresne, A.; Thomas, S.; Galeski, A. Recent developments in nanocellulose-based biodegradable polymers, thermoplastic polymers, and porous nanocomposites. *Prog. Polym. Sci.* 2018, 87, 197–227. [CrossRef] 186. Sun, Y.; Chu, Y.; Wu, W.; Xiao, H. Nanocellulose-based Lightweight Porous Materials: A Review. *Carbohydr. Polym.* 2021, 255, 117489. [CrossRef] 187. Zhao, J.; Lu, C.; He, X.; Zhang, X.; Zhang, W.; Zhang, X. Polyethylenimine-grafted cellulose nanofibril aerogels as versatile vehicles for drug delivery. *ACS Appl. Mater. Interfaces* 2015, 7, 2607–2615. [CrossRef] [PubMed] 188. Liang, Y.; Zhu, H.; Wang, L.; He, H.; Wang, S. Biocompatible smart cellulose nanofibres for sustained drug release via pH and temperature dual-responsive mechanism. *Carbohydr. Polym.* 2020, 249, 116876. [CrossRef] [PubMed] 189. Svagan, A.J.; Benjamins, J.-W.; Al-Ansari, Z.; Shalom, D.B.; Mullertz, A.; Wagberg, L.; Lobmann, K. Solid cellulose nanofiber based foams—towards facile design of sustained drug delivery systems. *J. Controlled Release* 2016, 244, 74–82. [CrossRef] [PubMed] 190. Lobmann, K.; Svagan, A.J. Cellulose nanofibers as excipient for the delivery of poorly soluble drugs. *Int. J. Pharm.* 2017, 533, 285–297. [CrossRef] [PubMed] 191. Svagan, A.J.; Mullertz, A.; Lobmann, K. Floating solid cellulose nanofibre nanofoams for sustained release of the poorly soluble model drug furosemide. *J. Pharm. Pharmacol.* 2017, 69, 1477–1484. [CrossRef] 192. Bannow, J.; Benjamins, J.-W.; Wohler, J.; Lobmann, K.; Svagan, A.J. Solid nanofoams based on cellulose nanofibers and indomethacin—The effect of processing parameters and drug content on material structure. *Int. J. Pharm.* 2017, 526, 291–299. [CrossRef] [PubMed] 193. Fiorati, A.; Turco, G.; Travan, A.; Caneva, E.; Pastori, N.; Cametti, M.; Punta, C.; Melone, L. Mechanical and drug release properties of sponges from cross-linked cellulose nanofibers. *ChemPlusChem* 2017, 82, 848–858. [CrossRef] [PubMed] 194. Xiao, Y.; Rong, L.; Wang, B.; Mao, Z.; Xu, H.; Zhong, Y.; Zhang, L.; Sui, X. A light-weight and high-efficacy antibacterial nanocellulose-based sponge via covalent immobilization of gentamicin. *Carbohydr. Polym.* 2018, 200, 595–601. [CrossRef] [PubMed] 195. Rahimi, M.; Shojaei, S.; Safa, K.D.; Ghasemi, Z.; Salehi, R.; Yousefi, B.; Shafiei-Irannejad, V. Biocompatible magnetic tris (2- aminoethyl) amine functionalized nanocrystalline cellulose as a novel nanocarrier for anticancer drug delivery of methotrexate. *New J. Chem.* 2017, 41, 2160–2168. [CrossRef] 196. Supramaniam, J.; Adnan, R.; Kaus, N.H.M.; Bushra, R. Magnetic nanocellulose alginate hydrogel beads as potential drug delivery system. *Int. J. Biol. Macromol.* 2018, 118, 640–648. [CrossRef] 197. Jeddi, M.K.; Mahkam, M. Magnetic nano carboxymethyl cellulose-alginate/chitosan hydrogel beads as biodegradable devices for controlled drug delivery. *Int. J. Biol. Macromol.* 2019, 135, 829–838. [CrossRef] 198. Cirillo, G.; Hampel, S.; Spizzirri, U.G.; Parisi, O.I.; Picci, N.; Iemma, F. Carbon nanotubes hybrid hydrogels in drug delivery: A perspective review. *BioMed Res. Int.* 2014, 825017. [CrossRef] 199. Zhang, W.; Zhang, Z.; Zhang, Y. The application of carbon nanotubes in target drug delivery systems for cancer therapies. *Nanoscale Res. Lett.* 2011, 6, 1–22. [CrossRef] [PubMed] 200. Anirudhan, T.; Shainy, F.; Thomas, J.P. Effect of dual stimuli-responsive dextran/nanocellulose polyelectrolyte complexes for chemo photothermal synergistic cancer therapy. *Int. J. Biol. Macromol.* 2019, 135, 776–789. *Polymers* 2021, 13, 2052 2 of 47 *Polymers* 2021, 13, 2052 3 of 47 *Polymers* 2021, 13, 2052 5 of 47 *Polymers* 2021, 13, 2052 6 of 47 *Polymers* 2021, 13, 2052 7 of 47 *Polymers* 2021, 13, 2052 8 of 47 *Polymers* 2021, 13, 2052 9 of 47 *Polymers* 2021, 13, 2052 10 of 47 *Polymers* 2021, 13, 2052 11 of 47 *Polymers* 2021, 13, 2052 12 of 47 *Polymers* 2021, 13, 2052 13 of 47 *Polymers* 2021, 13, 2052 14 of 47 *Polymers* 2021, 13, 2052 15 of 47 *Polymers* 2021, 13, 2052 16 of 47 *Polymers* 2021, 13, 2052 *Polymers* 2021, 13, 2052 18 of 47 18 of 49 *Polymers* 2021, 13, 2052 19 of 47 *Polymers* 2021, 13, 2052 20 of 47 *Polymers* 2021, 13, 2052 21 of 47 *Polymers* 2021, 13, 2052 22 of 47 *Polymers* 2021, 13, 2052 23 of 47 *Polymers* 2021, 13, 2052 24 of 47 *Polymers* 2021, 13, 2052 25 of 47 *Polymers* 2021, 13, 2052 26 of 47 *Polymers* 2021, 13, 2052 27 of 47 *Polymers* 2021, 13, 2052 28 of 47 *Polymers* 2021, 13, 2052 29 of 47 30 of 47 *Polymers* 2021, 13, 2052 *Polymers* 2021, 13, 2052 32 of 47 *Polymers* 2021, 13, 2052 33 of 47 *Polymers* 2021, 13, 2052 34 of 47 *Polymers* 2021, 13, 2052 35 of 47 *Polymers* 2021, 13, 2052 36 of 47 *Polymers* 2021, 13, 2052 37 of 47 *Polymers* 2021, 13, 2052 38 of 47 *Polymers* 2021, 13, 2052 39 of 47 *Polymers* 2021, 13, 2052 40 of 47 *Polymers* 2021, 13, 2052 41 of 47 *Polymers* 2021, 13, 2052 42 of 47 *Polymers* 2021, 13, 2052 43 of 47 *Polymers* 2021, 13, 2052 44 of 47 *Polymers* 2021, 13, 2052 45 of 47 *Polymers* 2021, 13, 2052 46 of 47 *Polymers* 2021, 13, 2052 47 of 47